# Pinning phenomena and critical currents in disordered long Josephson junctions

Roland Fehrenbacher
*Theoretische Physik, ETH-Hönggerberg, CH-8093 Zürich, Switzerland*

Vadim B. Geshkenbein
*Theoretische Physik, ETH-Hönggerberg, CH-8093 Zürich, Switzerland*
*and L.D. Landau Institute for Theoretical Physics, 117940 Moscow, U.S.S.R.*

Gianni Blatter
*Theoretische Physik, ETH-Hönggerberg, CH-8093 Zürich, Switzerland*
*and Asea Brown Boveri, Corporate Research, CH-5405 Baden, Switzerland*
(Received 26 September 1991)

The critical current $I_c$ of a long one-dimensional (1D) Josephson junction in the presence of different types of structural disorder is investigated both analytically and numerically. It is shown that most properties of $I_c$ can be understood from the behavior of the elementary pinning force (PF) of a single defect, which we calculate exactly as a function of the external magnetic field $H_e$, pinning-center size, and strength. The following types of disorder are discussed: (i) For a given field, and pinning centers with equal strength, a unique arrangement of pins that maximizes $I_c$ is found. (ii) In the case of a periodic pinning-center lattice, we reproduce the commensurability peaks in the field dependence of the critical current, $I_c(H_e)$, previously reported by Oboznov and Ustinov [Phys. Lett. A **139**, 481 (1989)]. In addition, we predict that a peak can be damped or disappear, if its position coincides with a field value at which the elementary PF vanishes. (iii) The most interesting effects appear in the presence of random disorder. Using the exact expression for the elementary PF, we extend the collective pinning analysis of Koshelev and Vinokur (Zh. Eksp. Teor. Fiz. **97**, 976 (1990) [Sov. Phys. JETP **70**, 547 (1990)]) to arbitrary fields and properties of the disorder, and compare the obtained predictions with the results of numerical simulations. The agreement between the two approaches is extremely good. In particular, we find that the appearance of a plateau in $I_c(H_e)$ for large fields depends strongly on the ratio $\bar{r}_0/\bar{\lambda}_j$ between the average pinning center size $\bar{r}_0$ and the average Josephson penetration depth $\bar{\lambda}_j$. If $\bar{r}_0/\bar{\lambda}_j \approx 1$, there is no plateau at all, and in the case $\bar{r}_0/\bar{\lambda}_j \ll 1$, a plateau is found up to fields for which the vortex spacing becomes of the order of $\bar{r}_0$. Furthermore, we predict the possibility of a dimensional crossover from a 1D behavior at low fields to 0D behavior at large fields. Finally, we present a possible explanation of the experimentally observed plateau in the $j_c(H_e)$ dependence of granular high-$T_c$ materials.

## I. INTRODUCTION

The interest in the physics of Josephson junctions has been unbroken since Josephson's predictions of the basic relations governing the tunneling of Cooper pairs across so-called weak links.[1] Most aspects of the observed phenomena are well understood by now, and numerous technical applications of the Josephson effects have been developed as a consequence.[2]

Soon after Josephson's discovery, it was realized that the self-field of the tunneling supercurrent introduces a typical screening length scale, the Josephson penetration depth $\lambda_j$, which leads to the occurrence of a *weak* Meissner effect for *long* Josephson junctions (LJJ) with length $L \gg \lambda_j$. Furthermore, there exists a critical field $H_{c_0}$ in LJJ, above which the magnetic field enters the sample in the form of Josephson vortices. These properties establish a certain correspondence between type-II superconductors and LJJ. In fact, a LJJ can be viewed as a dimensionally reduced type-II superconductor, exhibiting all the well-known phenomena such as a Meissner effect, topological (however, coreless) vortex excitations, pinning, and also a critical state.[3,4] A detailed study of the vortex state and the Meissner effect in homogeneous LJJ was done by Owen and Scalapino (OS). They determined the possible magnetic field and current distributions inside the junction, and calculated the field dependence of the critical current.[5] Their calculated curve was beautifully confirmed by experiment.[6]

For many technical applications of superconductors and LJJ, the ability to carry a nonzero critical current in considerably large applied magnetic fields is a key property. In the case of type-II superconductors, it is well known that the existence of a finite critical current in the mixed state is due to the pinning of the vortices at inhomogeneities of the sample. This prevents the dissipation arising from moving flux lines. Intuitively, one also expects that some kind of disorder-induced pinning should lead to an increase of the critical current exhibited by a LJJ, but the pinning phenomena are not very well understood. A first hint to the mechanism of pinning is

 

found when comparing the LJJ to the Josephson point contact (which has a length $L \ll \lambda_j$) for which the local magnetic field can be assumed to be uniform: The critical current of the point contact vanishes at fields corresponding to the penetration of an integer number of flux quanta $\Phi_0 = hc/2e$, whereas a homogeneous LJJ has a finite critical current at any field below the second critical field $H_{c_2}$ of the bulk superconductors, which are separated by the junction. The finite critical current of the LJJ arises from the pinning of the vortex lattice at the sharp boundaries of the junction, where the Josephson coupling abruptly drops to zero. Hence, the boundaries act as a defect, i.e., constitute a pinning potential. However, since the pinning due to the boundaries is a surface effect, the limit $\lim_{L\to\infty} I_c/L$ vanishes; i.e., the uniform LJJ *cannot carry a critical current density.* More generally, one can expect that an inhomogeneous coupling throughout the LJJ can lead to real bulk pinning.

Previous investigations of Josephson vortex pinning concentrated mainly on the case of a single defect or a periodical modulation of the Josephson coupling, with the center of interest being the question how the dynamics of the fluxons is affected by the disorder.[7] Another approach was chosen by Vasenko, Likharev, and Semenov,[8] who studied large-scale disorder of arbitrary kind, which allowed an analytical treatment by means of asymptotic methods. Unfortunately, these methods can only be applied if the length scale of the disorder is large compared to the vortex lattice (VL) spacing. In general, this is a severe restriction, but in the limit of sufficiently large magnetic fields their results should be applicable. They studied a junction for which the Josephson coupling goes smoothly to zero as one approaches the boundaries, which isolates the effect of bulk pinning from the surface pinning at the sharp boundaries of a uniform LJJ. The asymptotic decrease of the critical current for large external fields $H_e$ was found to be $\propto 1/H_e^2$, and their formula for $I_c$ was independent of the junction length $L$. Hence, they predict that the contribution of bulk pinning decreases faster than the critical current due to the surface pinning, i.e., for very large fields, an asymptotic decrease $I_c \propto 1/H_e$ (as for the homogeneous case) should be observed. Our analysis confirms this asymptotic decrease for large fields, however, we find a length dependence $I_c \propto L^{1/2}$ of the critical current.

Very recently, Vinokur and Koshelev (VK) were motivated by the possible relevance of disordered LJJ in the context of theories for polycrystalline high-$T_c$ materials.[9] They investigated the behavior of $j_c(H_e)$ at zero as well as nonzero temperature in the presence of random disorder by employing Larkin and Ovchinnikov's *collective pinning theory*[10] (CPT), which was originally developed and successfully applied to model random disorder in type-II superconductors. However, the analysis of the field dependence of $j_c$ by VK was only qualitative and relied on an approximation for the elementary pinning force (PF), which, as we shall show, can only be justified in a restricted field region, the size of which depends on the typical length scale $\bar{r}_0$ of the disorder. Their main result was the appearance of a plateau in the $j_c(H_e)$ characteristic for large fields, and they argued that this might explain the experimentally observed plateaus in polycrystalline high-$T_c$ materials.[11–13] We shall show that the field region for which a plateau exists actually depends on the ratio of $\bar{r}_0/\bar{\lambda}_j$ ($\bar{\lambda}_j$ is an average value), and that it *can be absent,* if this ratio is larger or of the order of 1. For a Josephson point contact, the influence of random disorder on the field-current characteristic was also found to yield a plateau for *small scale* disorder ($\bar{r}_0/L \ll 1$, $L \sim \bar{\lambda}_j$, where $\bar{r}_0$ is again the correlation length of the disorder and $L$ the junction length), and small external magnetic fields.[14,15] For large fields, a decreasing current $I_c$ was predicted.[14,15] This behavior is fully consistent with our results.

In this work, we concentrate on the static properties of the disordered LJJ. In particular, we are interested in the field dependence of the critical current about which, in our opinion, a detailed understanding for arbitrary fields and types of disorder is still lacking. Our investigations are based (i) on large-scale numerical simulations of the disordered LJJ, by exactly solving the *self-consistent* static sine-Gordon equation in the presence of a position-dependent coupling strength, and (ii) on improving the CPT approach of VK to the case of arbitrary fields and pinning-center sizes. The predictions of CPT can then be directly compared to the numerical results. In our simulations, the disorder in the LJJ is modeled by a piecewise constant coupling. This allows for a numerically obtained *exact* solution of the perturbed sine-Gordon equation and thus produces reliable results in the entire field regime and for arbitrary types of disorder. As an optical guide through the paper, in Figs. 1(a)–1(d), we show typical shapes of the local magnetic field and current density patterns at the critical current for a field $H_e/H_{c_0} = 5$. We compare a uniform junction [Fig. 1(a)] with junctions having different types of disorder, viz., optimized arrangement of defects [Fig. 1(b)], periodic defect lattice [Fig. 1(c)], and random defects [Fig. 1(d)].

Our motivation for studying the disordered LJJ also stems from the experimental picture found from magnetization and transport measurements on polycrystalline high-$T_c$ materials, which suggests modeling these materials as granular superconductors:[16] What was observed is a large difference between the critical currents responsible for transport ($\approx 10^2$–$10^3$ A/cm$^2$) and diamagnetism ($\approx 10^5$–$10^7$ A/cm$^2$), the latter being several orders of magnitude larger.[11–13] Furthermore, the transport critical currents showed a very strong field dependence with a sharp decrease (of one order of magnitude) at very low fields ($\approx$20–80 G) along with a strong weakening of the Meissner effect at roughly the same fields. One concludes that these fields correspond roughly to the average critical Josephson field $\bar{H}_{c_0}$. From all these properties, one can conclude, that the polycrystalline high-$T_c$ oxides should be modeled as an agglomeration of islands with strong superconductivity having their order parameters coupled via Josephson contacts. The large screening currents could then be attributed to the *strong intragrain,* and the transport currents to the *weak intergrain* superconductivity. Thus the critical transport current is essen-

tially limited by the depinning of the intergrain Josephson vortices. A study of the pinning properties of Josephson vortices should therefore yield valuable information about the behavior of the polycrystalline high-$T_c$ materials.

A realistic model for a *strongly* coupled granular superconductor was proposed by Rhyner and Blatter, and called the *limiting interface model.*[17] Within this model, the critical current of a sample is limited by the depinning of the Josephson vortices across a limiting interface of weakest superconductivity, which extends over the entire sample. Applied to the case of, e.g., a textured $YBa_2Cu_3O_{7-\delta}$ film, the interface actually becomes a critical path which represents a one-dimensional inhomogeneous, macroscopic LJJ. Therefore, the field dependence of the critical current of such a film should be given by the $j_c(H_e)$ dependence of the single LJJ. It is interesting to note, that for the case of Abrikosov vortices the vortex flow also seems to start along a critical path, as has recently been shown in a numerical simulation by Jensen *et al.*[18]

As an introduction to the disordered case, in Sec. II, we shall briefly review the static properties of a uniform LJJ, and also describe the numerical procedure used to simulate the field dependence of the critical current. At the end, we shall discuss some aspects of the LJJ, which are relevant for the disordered case.

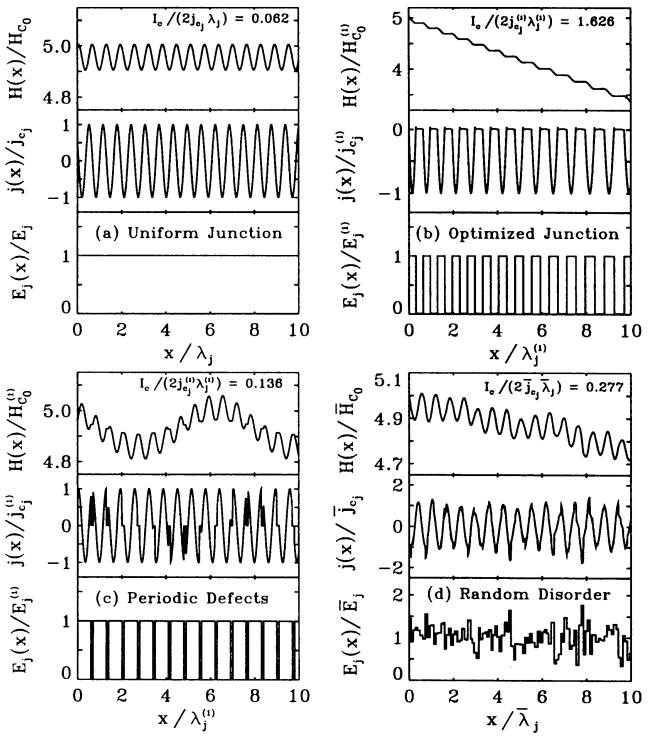


FIG. 1. Typical shapes of the local magnetic field $H(x)$, and the current density $j(x)$ at the critical current for LJJ's with different types of disorder characterized by the function $E_j(x)$ (in all cases the applied field was chosen as $H_e=5$ measured in units of $H_{c_0}$, $H_{c_0}^{(1)}$, and $\bar{H}_{c_0}$, respectively): (a) The uniform junction with ratio $L/\lambda_j=10$. (b) An optimized junction with $L/\lambda_j^{(1)}=10$ and $\lambda_j^{(1)}/\lambda_j^{(2)}=0.1$. (c) A periodically modulated junction with parameters $L/\lambda_j^{(1)}=10$, $d_p/\lambda_j^{(1)}=0.6$, $d_p/s_p=6$, and $\lambda_j^{(1)}/\lambda_j^{(2)}=0.1$. (d) A randomly disordered junction with parameters $L/\bar{\lambda}_j=10$, $q=0.09$, $\bar{r}_0/\bar{\lambda}_j=0.1$, and $\sigma_{r_0}/\bar{r}_0=0.2$.

In Sec. III, we calculate the elementary PF of a single defect *exactly.* It will be shown that, for a fixed size of the defect, the PF is a periodic function of the external field with zeros at points where the pinning center size is an integer multiple of the vortex spacing. As fluctuations of the defect sizes are turned on, these zeros change into minima. For very strong fluctuations, only the first minimum at the field where the mean pinning center size and the vortex distance coincide survives, whereas for larger fields the pinning force becomes constant. These results are applied to different types of disorder in Secs. IV–VI: first we discuss the construction of a junction with *maximum pinning* at a given external field. The critical current of such an optimized junction is strongly enhanced, and in fact, one finds a critical current density, which is of the order of the maximum Josephson critical current density $j_{c_j}$. The $j_c(H_e)$ curve shows a linear rise up to the field for which the junction is optimized, followed by a sharp drop reflecting only small pinning forces for larger fields.

For a periodic defect lattice, experimental $j_c(H_e)$ curves exist and show pronounced peaks at fields where the periods of the vortex and the defect lattice are commensurate.[19] Our numerical curves obtained for such junctions accurately reproduce these peaks. In addition, we argue that certain peaks will be totally suppressed if the ratio between the size of the defects and their distance is rational, because then the peak criterion coincides with the criterion for a vanishing PF. To our knowledge, such a junction has not been produced until now, and it would be interesting to check this prediction experimentally.

The case of main interest is random disorder. In Sec. VI, we compare our numerical results to the predictions obtained by applying CPT, where we use the results for the average elementary PF from Sec. III, and calculate the field dependence of the critical current density in the usual fashion. VK already predicted that the correlation length $L_c$, which in CPT determines the size of regions in the VL over which short-range order is preserved, substitutes the Josephson penetration depth in deciding about the effective dimensionality of the junction, i.e., junctions with length smaller than $L_c$ behave effectively like a point contact. We find the additional feature that $L_c$ is strongly field dependent for fields, which produce a vortex distance much smaller than the typical length scale $\bar{r}_0$ of the disorder. Therefore, in a junction that at low fields is effectively one-dimensional with a length $L>L_c$, a dimensional crossover can occur as the external field is increased.

The plateau in $j_c(H_e)$ which was believed by VK to be a generic feature of a disordered LJJ is shown to occur only when $\bar{r}_0$ is much smaller than the average Josephson penetration depth $\bar{\lambda}_j$, and even then, for strong enough fields a second drop is shown to occur. The appearance of the plateau, as well as such an additional drop is also

seen in the measured $j_c(H_e)$ of polycrystalline high-$T_c$ materials at fields well above $H_{c_1} \approx 500$ G of the grains. Whether or not the existence of Abrikosov vortices in the grains changes our results dramatically cannot be decided with certainty, but we believe that the basic physical picture should not be altered. The fields up to which a plateau is experimentally found in the granular high-$T_c$ materials are 3–4 orders of magnitude larger than the estimated value of the average Josephson critical field $\bar{H}_{c_0} \approx 20-80$ G (see above). From this it can be concluded that if the $j_c(H_e)$ dependence of the polycrystalline high-$T_c$ films or bulk superconductors is essentially determined by the depinning of the Josephson vortices along a critical path (interface) as suggested by the limiting path (interface) model, the disorder producing this plateau must vary on very small scales approximately three orders of magnitude smaller than $\bar{\lambda}_j$, which can be estimated to be a few $\mu$m.

The comparison of our numerical results with the predictions of CPT shows very good agreement. The numerically extractable dependencies of $j_c$ on the junction parameters and applied magnetic field are reproduced very impressively, and the numerical factor needed to obtain quantitative agreement between the two approaches is of order unity. In summary, CPT is found to yield a reliable qualitative description for the phenomena induced by random disorder in LJJ.

## II. THE UNIFORM LONG JOSEPHSON JUNCTION

In order to investigate the pinning of Josephson vortices in disordered junctions, it is important to have a thorough understanding of the physics of a *uniform* LJJ. In this section, we will briefly review the well-known work by Owen and Scalapino (OS) on this matter,[5] and in addition, we try to point out a few ideas that we believe to be central to the concept of pinning.

We consider a so-called "in-line asymmetrical" junction geometry (see Fig. 2) with the uniform applied magnetic field $H_e$ directed along the $y$ axis and the current flowing in the $z$ direction. The $y$ dimension $W$ of the contact is assumed to be very small compared to the Josephson penetration depth $\lambda_j$, which sets the length scale on which the physical quantities vary. Hence, variation is only allowed along the $x$ axis, and all the physical quantities are translationally invariant along the $y$ direction. Furthermore, we choose the length $L$ of the junction in $x$ direction to be much larger than $\lambda_j$, thus arriving at a one-dimensional LJJ.

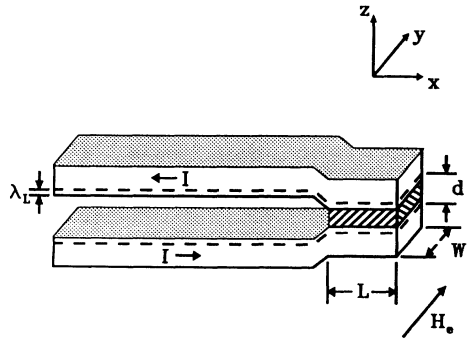


FIG. 2. The geometry of the "in-line asymmetrical" LJJ.

The basic equations governing the physics of the LJJ are (1a), Josephsons relation between the tunneling supercurrent $j(x)$ and the relative pair phase $\Theta(x)$, and (1b), the proportionality of the phase gradient to the local magnetic field $H(x)$:

$$j(x)=j_{c_j}\sin\Theta(x) , \tag{1a}$$

$$\frac{\partial\Theta}{\partial x}=\frac{2ed}{\hbar c}H(x) , \tag{1b}$$

where $j_{c_j}$ is the maximal Josephson current density, $d=2\lambda_L+\epsilon$, with $\lambda_L$ the London penetration depth, and $\epsilon$ is the insulator thickness. Combining (1a) and (1b) with Maxwell's equations yields the familiar pendulum equation (or stationary sine-Gordon equation)

$$\frac{\partial^2}{\partial x^2}\Theta(x)=\frac{1}{\lambda_j^2}\sin\Theta(x) , \tag{2}$$

where the penetration depth is determined by $\lambda_j^2=\hbar c^2/(8\pi e d j_{c_j})$. Note that allowing for a finite voltage drop across the junction would lead to additional terms with time derivatives in (2), so we are restricting ourselves to *stationary* field and current distributions. In order to uniquely specify a solution of (2), one needs a set of boundary conditions that are determined by the junction geometry and for our case read[20]

$$H(x=0)=H_e-\frac{4\pi}{c}I , \tag{3a}$$

$$H(x=L)=H_e . \tag{3b}$$

Here we have introduced the total current $I$ which from Ampères law becomes

$$I=W\int_0^L j(x)dx=\frac{c}{4\pi}W[H(L)-H(0)] .$$

In the following, we shall set the width $W=1$. Note that these boundary conditions are different from the symmetric ones used by OS. However, since the effect of bulk pinning is not affected by the boundary conditions, we are guided here by pure computational convenience when making our choice, as will become clear later.

A first point to note about the "equation of motion" (2) is the fact that it has an important integral (corresponding to the conserved total energy of the pendulum), viz.,

$$\kappa=\left[\left[\frac{\lambda_j}{2}\frac{\partial\Theta}{\partial x}\right]^2+\cos^2\left[\frac{\Theta}{2}\right]\right]^{-1/2} . \tag{4}$$

It turns out that apart from a translation, this parameter completely determines a solution of (2). Depending on whether $\kappa \geq 1$, or $\kappa < 1$ there are *two* types of solutions, both of which can be expressed in terms of Jacobian elliptic functions,[21]

$$\kappa>1 \qquad\qquad \kappa<1$$

$$\sin\left[\frac{\Theta(x)}{2}\right]=\mathrm{sn}\left[\frac{x-x_0}{\lambda_j}\middle|\frac{1}{\kappa^2}\right], \qquad \sin\left[\frac{\Theta(x)}{2}\right]=\mathrm{cn}\left[\frac{x-x_0}{\kappa\lambda_j}\middle|\kappa^2\right] \tag{5a}$$

$$\frac{2ed}{\hbar c}H(x)=\frac{\partial\Theta}{\partial x}=\frac{2}{\kappa\lambda_j}\mathrm{cn}\left[\frac{x-x_0}{\lambda_j}\middle|\frac{1}{\kappa^2}\right], \quad \frac{2ed}{\hbar c}H(x)=\frac{\partial\Theta}{\partial x}=\frac{2}{\kappa\lambda_j}\mathrm{dn}\left[\frac{x-x_0}{\kappa\lambda_j}\middle|\kappa^2\right]. \tag{5b}$$

The critical value $\kappa_c=1$ has an important physical significance: solutions with $\kappa>\kappa_c$ can only occur for applied fields below $H_{c_0}=\hbar c/(ed\lambda_j)$. In fact, this critical field corresponds to the usual first critical field $H_{c_1}$ of a bulk type-II superconductor, since only below $H_{c_0}$, i.e., for $\kappa>\kappa_c$, there exist solutions which describe the shielding of the magnetic field from the interior of the junction, i.e., a Meissner effect with effective screening length $\lambda_j$, the Josephson penetration depth. For fields above $H_{c_0}$, the only possible solutions have $\kappa<\kappa_c$, and they describe configurations where the magnetic field has penetrated into the sample in the form of Josephson vortices.

In spite of the apparent analogy between a bulk type-II superconductor and a LJJ, there are important differences between Josephson and Abrikosov vortices: Josephson vortices involve *one single* length scale $\lambda_j$, whereas an Abrikosov vortex is characterized by two lengths, the coherence length $\xi$ (characterizing the core), and the London penetration depth $\lambda_L$ (characterizing electromagnetic properties). Abrikosov vortices have a well-defined *normal* core at which the superconducting order parameter vanishes. In contrast, Josephson vortices have *no normal core* whatsoever (the modulus of the superconducting order parameter essentially vanishes inside the whole junction). The basic property of a Josephson vortex is a rapid change of the order parameter *phase* by $2\pi$. The position of a Josephson vortex can be accurately defined as the point at which the phase derivative, i.e., the local magnetic field, has a maximum, and the vortex spacing is determined by the periodicity $a$ in the solutions (5a) and (5b) for $\kappa<1$. It is given by $a=2\lambda_j\kappa K(\kappa^2)$, which approaches the asymptotic value $a_\infty\propto\pi\lambda_j H_{c_0}/H_e$ for large fields $H_e\gg H_{c_0}$. Here $K(\kappa^2)$ is the complete elliptic integral of the first kind.[21]

Until now, we have considered general solutions of (2), but in reality we are interested in only one of them, the one which produces the largest current. This will be the critical current of the junction because the solutions of (2) describe all possible stationary configurations, whereas nonstationary ones would lead to dissipation and are thus overcritical. The computational strategy for finding the critical current is as follows (note the difference to OS): Fix the magnetic field $H(L)=H_e$ and the phase $\Theta(L)=\Theta_0$ at the outer end of the junction. This determines the value of $\kappa$ via (4), i.e., the shape of the VL, and using the boundary conditions (3) at $x=L$, the shift $x_0$ in the solutions (5a) and (5b), i.e., the VL position, is also fixed. Hence, we have completely determined the solution by specifying the pair $H_e,\Theta_0$. We can now calculate the value of the magnetic field at the other end of the junction and obtain the total current $I(H_e,\Theta_0)$ of this particular solution. Finding the *critical* current $I_c(H_e)$ now simply becomes an optimization problem for the function $I(H_e,\Theta_0)$ with respect to $\Theta_0$, such that

$$I_c(H_e)=\max_{-\pi\le\Theta_0\le\pi}|I(H_e,\Theta_0)| .$$

Before graphically showing the field dependence of the critical current, let us mention a few general properties of the uniform LJJ: From the solutions (5a) and (5b), one can readily determine the asymptotic behavior of $I_c(H_e)$. Since for large fields, the phase dependent term in (4) becomes negligible, the asymptotic value for $\kappa$ is $\kappa_\infty=H_{c_0}/H_e$, and hence, the oscillation amplitude $\Delta H$ of

$$H(x)\propto\mathrm{dn}[x-x_0/(\kappa_\infty\lambda_j)|\kappa_\infty^2]/\kappa_\infty$$

is an upper bound for the field difference at the two ends of the junction. In the asymptotic regime this oscillation amplitude becomes

$$\Delta H/H_{c_0}=\kappa_\infty/2=H_{c_0}/(2H_e) ,$$

and hence, the upper bound for $I_c$ is

$$I_c\le(c/4\pi)\Delta H=(c/8\pi)H_{c_0}^2(1/H_e) .$$

So the envelope of the $I_c(H_e)$ curve decreases as $1/H_e$ for large fields, which can be seen in Fig. 3. The small oscillations of $I_c(H_e)$ in Fig. 3 are due to the formation of one additional vortex and correspond to the zeros in the Fraunhofer pattern of a short Josephson junction, which result from the penetration of one additional flux quan-

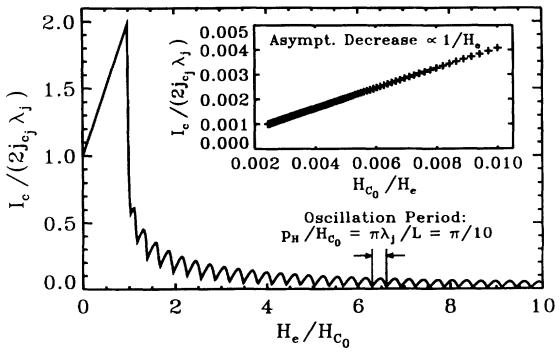


FIG. 3. The field dependence of the critical current, $I_c(H_e)$, of the uniform junction mentioned in Fig. 1(a). The small oscillations correspond to the penetration of one additional vortex. The window shows a plot of $I_c$ as a function of the inverse applied field $H_{c_0}/H_e$. One observes a straight line, indicating the asymptotic law $I_c\propto 1/H_e$.

tum $\Phi_0$. The period of these oscillations depends on the length of the LJJ and is given by $p_H=\pi\lambda_j H_{c_0}/L$. The shapes of $j(x)$ and $H(x)$ at the critical current for a field $H_e/H_{c_0}=5$ is shown in Fig. 1(a).

The last property of the uniform LJJ we would like to mention is the fact that it cannot carry a critical current *density* $j_c$. The total current through the junction is always restricted to the junction surface, since the net current carried by a complete vortex vanishes. Incomplete vortices, however, can only appear at the surface; hence, we have a surface current and one can say that the existence of a nonzero $I_c$ at $H_e>H_{c_0}$ is due to the pinning of the VL at the surface, i.e., the surface acts as a defect. This idea can already give us a hint how we can achieve a larger $I_c$ and even a finite critical current density: The *key* to pinning in LJJ is to break the translational symmetry of the vortices by introducing disorder. In this way, one can make *each* vortex carry a net current, thus the total current is proportional to the number of vortices, which in turn is proportional to the junction length $L$, and we end up with a critical current density. Of course, the details of the behavior of $I_c$ and $j_c$ depend on the type of disorder, as we shall see in the following sections. The basic mechanism of pinning is, however, already explained by the above statement.

In order to be able to investigate pinning, we need to introduce a few more concepts: Pinning and PF's are best understood in terms of the pinning potential, which is defined from the total energy functional of the junction,

$$E(\Theta(x))=\int_0^L\left\{\bar{E}_j\left[\frac{\bar{\lambda}_j^2}{2}\left[\frac{\partial\Theta}{\partial x}\right]^2+1-\cos\Theta(x)\right]+V_p(x)[1-\cos\Theta(x)]\right\}dx\ , \tag{6a}$$

where $\bar{E}_j=\hbar\bar{j}_{c_j}/2e$ is the uniform Josephson coupling energy, and the term $\propto V_p(x)$ describes the nonuniformity, i.e., the pinning potential, which is zero for the uniform case. The equation of motion (2) can be derived from (6) by an Euler-Lagrange variational principle.

The way we have introduced the disorder in (6) corresponds to a situation where the coupling energy $E_j(x)=\bar{E}_j+V_p(x)$ becomes inhomogeneous via its dependence on $j_{c_j}(x)=\bar{j}_{c_j}+j_{c_j}^p(x)$, such that the penetration depth will also show spatial fluctuations according to $\lambda_j^2(x)\propto 1/j_{c_j}(x)$. The functional (6) can be rewritten in terms of $E_j(x)$ and $\lambda_j^2(x)$ as

$$E[\Theta(x)]=\int_0^L E_j(x)\left[\frac{\lambda_j^2(x)}{2}\left[\frac{\partial\Theta}{\partial x}\right]^2+1-\cos\Theta(x)\right]dx\ . \tag{6b}$$

As a consequence of the position dependence of the parameter $\lambda_j=\lambda_j(x)$, the solutions of the second-order nonlinear differential equation (2) can no more be expressed in closed analytical form. This means, that for a general function $\lambda_j(x)$, one can only obtain *approximate numerical* solutions. However, since we know the analytical solutions for constant $\lambda_j$, it becomes possible to obtain *exact* numerical solutions of (2) by choosing $\lambda_j(x)$ to be a piecewise constant function. In this way, one can approximate basically any smooth function $\lambda_j(x)$ arbitrarily well. For this choice of disorder, one can show that at the boundary $x_B$ between two regions with different constant $\lambda_j$ the phase $\Theta(x_B)$ and its derivative $\Theta'(x_B)\propto H(x_B)$ must be continuous, whereas the current density jumps according to Eq. (1a). Thus the solutions are simply obtained by propagating $\Theta(x)$ across regions with constant $\lambda_j$ via (5a) and (5b) and then use the continuity of $\Theta,\Theta'$ to obtain the solution for the next region. This procedure can be conveniently performed numerically. We have thus a reliable method for dealing with disorder in a LJJ and the algorithm for obtaining the critical current is the same as in the uniform case.

The dependence of $I(H_e,\Theta_0)$ on $\Theta_0$ is very smooth for a uniform junction, so the optimization, which has to be performed in order to obtain the critical current is not very difficult. This feature is drastically changed when disorder is introduced: $I(H_e,\Theta_0)$ varies on very small scales as a function of the initial value $\Theta_0$, and a huge number of maxima and minima appear. This indicates the existence of *chaotic behavior* in the dynamical system under consideration, since the features of solutions with almost identical starting conditions can be completely different. Numerically this presents a big problem because it is very time consuming to determine a global maximum in the presence of hundreds of local minima. However, we observe, that many different maxima are *almost degenerate,* so that it is not necessary to find the absolute maxima. This fact allows us to use a much faster nondeterministic optimization procedure similar to the simulated annealing algorithm.[22] As a check of the method, for some examples, the such obtained values of $I_c$ are compared with the real global maxima, and a relative error of less than 1% is found.

Before proceeding with the investigation of junctions with macroscopic disorder, i.e., many defects, we need to understand the pinning behavior of a *single* defect more deeply, and this will be our task in the following section.

## III. ELEMENTARY PINNING FORCE OF A SINGLE DEFECT

The one-dimensionality of the model we consider brings with it the nice feature that we can fairly easily calculate the pinning force of a single defect *exactly.* This is very useful because it turns out that many of the properties of a particular arrangement of defects (such as, e.g., random or periodic pinning centers) are already determined by the dependence of the elementary pinning force on the given parameters. To calculate this pinning force, one needs to obtain the change in potential energy of the VL due to the defect, i.e., the *pinning potential* $U_p$

and then differentiate $U_p$ with respect to the VL position $x_0$, which is defined from the solutions (5a) and (5b). The pinning force is thus given by $F_p=-\partial U_p(x_0)/\partial x_0$. In correspondence to a piecewise constant $E_j(x)$, which is used in the simulations, the type of defect we shall consider is simply a potential well in the Josephson coupling energy, i.e.,

$$E_j(x)=\bar{E}_j+V_p(x) ,$$

$$V_p(x)=\begin{cases}0, & x<0\\ -q^{1/2}\bar{E}_j, & \le x\le r_0\\ 0, & x>r_0 ,\end{cases}$$

where the dimensionless parameter $q$ describes the strength of the pinning potential. The pinning force for a more general shape of the defect should not behave qualitatively different.

Since we are mainly interested in the field dependence of the critical current above $H_{c_0}$, we perform the calculation of the elementary PF for flux lattices, which are described by a phase distribution $\Theta(x)$ with

$$\sin[\Theta(x)/2]=\mathrm{cn}(x-x_0/\kappa\lambda_j|\kappa^2)$$

and $\kappa<1$ [see Eq. (5a)]. So the VL position is determined by $x_0$, and the vortex density by the elliptic parameter $\kappa^2$. In this case, the (normalized) pinning potential $\tilde{U}_p=U_p/q^{1/2}\bar{E}_j$ can be written as [see Eq. (6a)]

$$\tilde{U}_p=-\int_0^{r_0}[1-\cos\Theta(x)]dx=-2\int_0^{r_0}\sin^2\left[\frac{\Theta(x)}{2}\right]dx=-2\lambda_j\kappa\int_{-x_0'/\kappa}^{(r_0'-x_0')/\kappa}\mathrm{cn}^2(s|\kappa^2)ds , \tag{7}$$

where $r_0'=r_0/\lambda_j$ and $x_0'=x_0/\lambda_j$. The resulting pinning force is then given by

$$\tilde{F}_p=\frac{F_p}{q^{1/2}\bar{E}_j}=-\frac{1}{\lambda_j}\frac{\partial}{\partial x_0'}\tilde{U}_p(x_0',r_0')=2\left[\mathrm{cn}^2\left[\frac{x_0'}{\kappa}\middle|\kappa^2\right]-\mathrm{cn}^2\left[\frac{r_0'-x_0'}{\kappa}\middle|\kappa^2\right]\right] \tag{8}$$

This function has the same spatial periodicity $a$ as the original vortex lattice indicating that the effective pinning potential varies typically on scales of the order of $a$. For a defect *lattice*, the parameter $x_0'$, which determines the strength and direction of the PF for any particular pin, will in general depend on the pinning center position and therefore be different for different pinning centers (an exception is, e.g., a periodic defect lattice at special values of the applied field, which we shall deal with in Sec. V). This problem always shows up in pinning theories and to resolve it, one needs a prescription (*summation rule*), which treats the effect correctly according to the type of pinning center configurations under consideration. An example of such a summation rule is the above mentioned "collective pinning theory,"[10] which describes random disorder assuming that the average total PF vanishes, and that the effective PF is due to fluctuations (see Sec. VI).

In any case if we want to use (8) for the summation process, we have to average out the VL position, by integrating the absolute value of $\tilde{F}_p$ over a period in $x_0'$. We can avoid taking the modulus, by simply choosing a half period in $x_0'$, e.g., $[r_0'/2, r_0'/2+\kappa K(\kappa^2)]$ [$K(\kappa^2)$ is again the complete elliptic integral of the first kind], on which $\tilde{F}_p$ does not change sign, thus obtaining

$$\hat{F}_p=\langle\tilde{F}_p\rangle_{x_0'}=\frac{2}{\kappa K(\kappa^2)}\int_{r_0'/2}^{r_0'/2+\kappa K(\kappa^2)}\left[\mathrm{cn}^2\left[\frac{x_0'}{\kappa}\middle|\kappa^2\right]-\mathrm{cn}^2\left[\frac{r_0'-x_0'}{\kappa}\middle|\kappa^2\right]\right]dx_0'$$

$$=\frac{4}{K(\kappa^2)}\frac{\mathrm{sn}\left[\frac{r_0'}{2\kappa}\middle|\kappa^2\right]\mathrm{cn}\left[\frac{r_0'}{2\kappa}\middle|\kappa^2\right]}{\mathrm{dn}\left[\frac{r_0'}{2\kappa}\middle|\kappa^2\right]}\approx\frac{4}{\pi}\sin(r_0'/\kappa)\quad(\text{for }\kappa\ll1) . \tag{9}$$

The result is an odd periodic function in $r_0'$, with zeros at points for which $r_0'=m2\kappa K(\kappa^2)$ ($m=1,2,3,\ldots$). At large fields, $\tilde{F}_p$ is also approximately periodic (in the asymptotic sense) in $1/\kappa$, i.e., in the applied field $H_e$. This means that for a fixed size of the pinning center, its force on the VL vanishes for certain fields. Since the vortex spacing corresponding to a given value of $\kappa$, i.e., applied field, is $a=2\lambda_j\kappa K(\kappa^2)$, this result is to be expected because the above condition simply states that the pinning center accommodates *exactly* $m$ vortices. But we know that the contribution to the pinning potential of a complete vortex inside the pinning center is zero [see Eq. (8)], so the same applies to any integral number of vortices resulting in a vanishing PF.

This behavior has an important consequence for the $j_c(H_e)$ characteristic of a junction with random disorder: If the defects are randomly distributed but have equal size, there should be sharp minima in the $j_c(H_e)$ curve with a critical current, which is of the order of the value in the corresponding uniform junction. However, if the sizes of the defects are also random, these minima should still appear, but be smoothed out more or less strongly,

depending on the broadness of the statistical distribution of the sizes. In fact, these different minima can be nicely identified in the simulations of junctions with the corresponding type of disorder (see Fig. 12).

The smoothing of the minima for cases with a random distribution of pinning center sizes can be obtained from $\hat{F}_p$ by taking the weighted average over $r_0'$, which we assume to be a Gaussian random variable with mean $\bar{r}_0'$ and variance $\sigma_r$,

$$\bar{F}_p = \frac{1}{N_r} \int_0^\infty e^{-(r_0'-\bar{r}_0')^2/2\sigma_r^2} |\hat{F}_p(r_0')| dr_0' , \tag{10}$$

where $N_r$ is the normalization integral

$$N_r = \int_0^\infty \exp[-(r_0'-\bar{r}_0')^2/2\sigma_r^2] dr_0' .$$

The integral Eq. (10) can only be calculated numerically, and the resulting behavior of $\bar{F}_p$ as a function of $1/\kappa$ and $\sigma_r$ with fixed $\bar{r}_0'=0.1$ is shown as a surface plot in Fig. 4. For finite $\sigma_r$, and large values of

$$1/\kappa \propto H_e/H_{c_0} > H_\sigma/H_{c_0} = \pi/\sigma_r ,$$

the PF becomes essentially constant because then there are many oscillations of $\hat{F}_p$ under the peak of the Gaussian at $\bar{r}_0'$. In Fig. 4, it can be observed that the field $H_\sigma$ is shifted to smaller and smaller values as $\sigma_r$ is increased, and for large values $\sigma_r/\bar{r}_0' > 0.18$ only the first and second oscillation of the unaveraged pinning force $\hat{F}_p$ survive.

The size-averaged expression $\bar{F}_p$ for the PF will enter our collective pinning analysis in Sec. VI, and we shall see that the behavior of $\bar{F}_p$ alone determines many of the features of the critical current. In the following, we shall use the results of this section to understand the dependence of the critical current on the applied field for different types of disordered junctions.

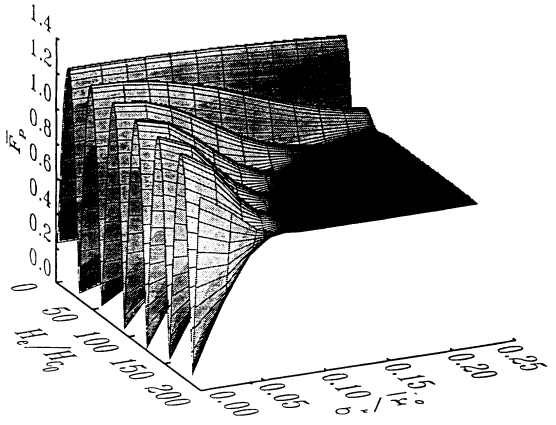


FIG. 4. The averaged pinning force $\bar{F}_p$ of a single defect as a function of the parameter $\kappa^{-1}(\propto H_e/H_{c_0}$ for $H_e/H_{c_0} \gg 1)$, and the degree of randomness of the distribution of the pin size, $\sigma_r/\bar{r}_0'$. The average pinning center size is chosen as $\bar{r}_0/\bar{\lambda}_j=0.1$. As the randomness is turned on, the oscillatory structure of $\bar{F}_p$ found for fixed pinning center size $(\sigma_r/\bar{r}_0'=0)$ is smoothed out, and for large fields, $\bar{F}_p$ approaches a constant. For $\sigma_r/\bar{r}_0' \geq 0.2$, only the first minima at the field where the average pinning center size $\bar{r}_0$ is equal to the vortex spacing $a$ survives. The regime of constant pinning force corresponds to the asymptotic decrease of the critical current stated in Eqs. (18).

## IV. OPTIMAL PINNING

In the last section, we have seen how the PF of a single defect depends on its size and the position of the VL. So one is led to ask the question whether there could be some kind of defect structure, which would produce a coherent addition of the PF of each single vortex, resulting in a strongly enhanced supercurrent. Remembering that the shape of the VL and in particular the distance between the vortices depends on the field strength, it becomes clear that the coherent PF addition would only be possible for certain external fields, because one requires the *matching* between the VL and the defect lattice. Furthermore, since a large critical current corresponds to a large field gradient across the sample, there will also be a vortex density gradient to which the defects have to adjust and therefore, the optimal defect lattice *cannot* be periodic.

In fact, it turns out that the determination of such an optimized junction is possible and also quite simple: Given two possible coupling strengths $E_j^{(1)}, E_j^{(2)}$ with $E_j^{(1)} \gg E_j^{(2)}$ (regions with $E_j^{(2)}$ represent strong pinning centers), we shall construct a junction of length $L$ characterized by an alternating piecewise constant $j_{c_j}$ according to the above couplings such that its critical current is maximal for a given external field. So within the class of disorder which can be represented by a step function in $j_{c_j}$, and under the additional restriction of only two possible coupling strengths, there exists a unique realization of disorder which exhibits maximal pinning. We shall also show that, in contrast to the uniform case, such a junction is able to carry a critical current density which is of the order of the larger $j_{c_j}^{(1)}$.

In the following, we will briefly describe how an optimized junction can be "constructed": Fix the external field $h_e=H_e/H_{c_0}^{(1)} \gg 1$ [from now on, a lowercase $h$ will always represent a magnetic field measured in units of $H_{c_0}^{(1)}=\hbar c/(ed\lambda_j^{(1)})$], and choose the first region to have large coupling $E_j^{(1)}$. The size of this region is determined by the requirement that the ratio $|I_1|/l_1$ of its total current and length be maximal. It is not difficult to see that this condition can be satisfied by choosing (i) the phase $\Theta(L)=\pi$ such that $j(L)=0$, $\kappa_1=1/h_e$ and (ii) $l_1$ to be exactly half of the corresponding vortex spacing, $l_1=a/2=\lambda_j^{(1)}K(1/h_e^2)/h_e$. This choice means that the first region is occupied by exactly half a vortex in such a way that the resulting current density points in the same direction everywhere between its zeros at $x_{c_0}=L$ and $x_{c_1}=L-l_1$, with $\Theta(x_{c_1})=2\pi$. It is now unavoidable to obtain a current in the opposite direction from the other half of the vortex, but this contribution can be made very small by choosing a small coupling $E_j^{(2)}$ for the next region. The length $l_2$ is calculated from the requirement

that $\Theta(x_{c_2})=\pi$, $j(x_{c_2})=0$ with $x_{c_2}=L-l_1-l_2$, which is the end point of the first vortex. Explicitly carrying out the calculation, one obtains $l_2=\kappa_2\lambda_j^{(2)}K(\kappa_2^2)$, where $\kappa_2=(h_e^2/q_j-1/q_j+1)^{-1/2}$ with the ratio $q_j=E_j^{(2)}/E_j^{(1)}\ll 1$. After this cycle, the field is lowered to the value $h(x_{c_2})=[h_e^2-(1-q_j)]^{1/2}$ yielding a total current of

$$I_1=\frac{c}{4\pi}[H(L)-H(x_{c_2})]$$
$$=\frac{c}{4\pi}H_{c_0}^{(1)}\{h_e-[h_e^2-(1-q_j)]^{1/2}\}\ . \qquad (11)$$

The same procedure can now be repeated $n$ times until (i) the end of the junction is reached with a total current

$$I_c=\sum_{i=1}^{n}I_n+\Delta I$$
$$=\frac{c}{4\pi}H_{c_0}^{(1)}\{h_e-[h_e^2-n(1-q_j)]^{1/2}\}+\Delta I\ .$$

where $\Delta I\ll I_c$ is the current of the last uncompleted cycle, or (ii) $h(x_{c_{2n}})<1$. If $h(x_{c_{2n}})<1$ occurs, then in the next cycle, the local magnetic field will change its direction. The optimization of this cycle is more difficult than for the previous ones, but still possible. However, since we are mainly interested in the limit of very long junctions with many cycles, the contribution of a single cycle is a $1/n$ effect. So we arbitrarily choose it to be symmetric which means that the length $l_{2n+1}$ corresponds to half a vortex with coupling $E_j^{(2)}$, $l_{2n+2}$ to half a vortex with $E_j^{(1)}$ (in which $h$ changes sign and $\kappa>1$) and then $l_{2n+3}$ to half a vortex with $E_j^{(2)}$. After this "turning," we can proceed like before until the end of the junction.

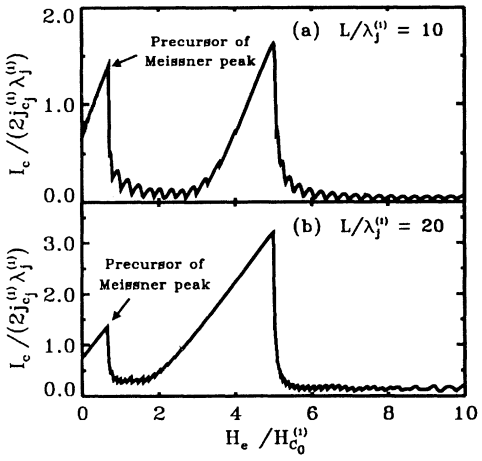


FIG. 5. The field dependence of the critical current, $I_c(H_e)$, of two optimized junctions with parameters $\lambda_j^{(1)}/\lambda_j^{(2)}=0.1$, and different lengths, (a) $L/\lambda_j^{(1)}=10$, (b) $L/\lambda_j^{(1)}=20$. A precursor of the Meissner-peak appears at a field $H_e/H_{c_0}<1$, followed by a usual sharp drop, and then a linear rise sets in up to the field $H_{\rm opt}$, for which the junction was optimized. At $H_{\rm opt}$, the critical current of junction (b) is exactly twice as large as the one of junction (a), confirming the existence of a critical current density.

In practice, this construction is most conveniently performed on the computer and in Figs. 5(a) and 5(b), we show the calculated field dependence of the critical current for a junction that was optimized for a field value $h_{\rm opt}=5$ using the following ratios for the total length and the penetration depths $L/\lambda_j^{(1)}=10,20$, and $\lambda_j^{(2)}/\lambda_j^{(1)}=10$. This particular geometry does not involve a "turning" cycle. One observes that a precursor of the usual peak at $H_e=H_{c_0}^{(1)}$ still appears at a slightly smaller value than $H_{c_0}^{(1)}$, but then a linear increase of $I_c$ sets in up to the field $H_e=H_{\rm opt}$, after which there is a very sharp drop to values which are of the same order of magnitude as the one found for the corresponding uniform junction. This drop means that the pinning for values above $H_{\rm opt}$ is weak.

The linear rise of $I_c$ can be qualitatively explained as follows: As $H_e<H_{\rm opt}$, the propagation of the solutions (5a) and (5b) in the regions where the defect sizes are smaller than half of the vortex, $a/2$, is nearly unaffected by the presence of the defects since there is no matching. As the solutions reach the region where $a/2$ becomes equal to the defect size, the initial phase $\Theta_0$ can be adjusted so that the VL can *lock into* the remaining part of the defect structure. In this way, a coherent PF addition is established over some fraction $L_{\rm com}$ of the sample and one can show that this fraction $L_{\rm com}$ grows linearly with the field, resulting in a corresponding linear increase of $I_c\approx j_c^{\rm opt}L_{\rm com}$, where $j_c^{\rm opt}$ is the averaged critical current density of the optimized junction.

The asymptotic value of $j_c^{\rm opt}$ for large fields can easily be calculated from the asymptotic form of the solutions (5a) and (5b): This asymptotic value is defined by $j_c^{\rm opt}=(c/4\pi)(\Delta H/\Delta L)$, where $\Delta H$ is the field difference from one cycle (vortex) for large fields $h\gg 1$ and $\Delta L$ its length. In this limit, one obtains

$$\Delta H\approx(cH_{c_0}^{(1)}/4\pi)(1-q_j)/(2h)$$

and $\Delta L\approx\lambda_j^{(1)}\pi/h$ so that the averaged current density becomes

$$j_c^{\rm opt}=\frac{1}{\pi}j_{c_j}^{(1)}\ . \qquad (12)$$

Note that the maximum critical current density is of the same order as $j_{c_j}^{(1)}$ and that it is *independent* of the field $h_{\rm opt}$ for which the junction was optimized. Fig. 1(b) shows the coupling $E_j(x)$, as well as the local field, and current density distribution for the above mentioned junction with length $L/\lambda_j^{(1)}=10$ at the critical current for applied field $H_e=H_{\rm opt}$. One can clearly see the average linear behavior of the local field corresponding to the constant $j_c^{\rm opt}$ across the junction. This field distribution is a direct analogue to the critical state in type-II superconductors.[3]

At first sight, the "construction" of such a junction looks like an academic problem, but, since the progress in device fabrication technology moves very fast, its experimental verification seems not impossible. A possible ap-

plication, for example, could be achieved by employing the drastic drop in $I_c$ to design a magnetic field driven electronic switch or a current limiter.

Another type of disorder, which has already been studied experimentally and theoretically, is that of a periodic defect lattice. In the next section, we will show that it is again a commensurability effect (but of a slightly different nature), which is responsible for the vortex pinning in such structures.

## V. PERIODIC DEFECT LATTICE

The pinning effect of a periodic defect lattice has been studied theoretically by various authors[7] using analytical approximation schemes like perturbation expansions[23] and variational methods.[24] Most of the approaches studied the dynamic behavior of the junction, and the main effort was directed to obtain the disorder-induced properties of the current-voltage characteristic of the junctions. Here we are interested in the field dependence of the critical current for a junction with a periodic pinning center lattice. Experimentally, the $I_c(H_e)$ curve of such a junction has been measured, and the main feature, which is the appearance of interference peaks was qualitatively explained by a simple commensurability criterion between the periods of the VL and the defect lattice.[19]

Our numerical investigations aim at reproducing the experimental curve and at providing a deeper understanding of the pinning mechanism responsible for it. In addition, our numerical study reveals a few new features of periodic pinning, such as the presence or absence of peaks in $I_c(H_e)$, depending on the size of the pinning centers, and we find that basically all the numerical results can be explained using the commensurability criterion and the behavior of the elementary PF as calculated in Sec. III.

In general, the interplay of two spatially periodic systems is always accompanied by some commensurability effects. In our case, the two systems are the periodic *soft* VL and the periodic *rigid* defect lattice. The interaction between the two can, of course, only affect the structure of the soft VL, which tries to adjust to the periodicity of the defects in order to maximize the PF's. This results in a periodic modulation of the vortex density [see Fig. 1(c)], which can be viewed as a supersoliton.[25] If the periods of the two lattices are incommensurate, the modulation wavelength $\lambda_m$ is very short (a few vortex spacings), and the modulation amplitude small, whereas in the commensurate case, the amplitude and the wavelength can become large (many vortex spacings).[26] As a consequence of this, at fields for which the VL becomes commensurate with the defect lattice, sharp peaks in the $I_c(H_e)$ curve can be observed.

In our numerical investigations, we model the periodic defects again by a step function consisting of a periodic chain of regions with alternating couplings $E_j^{(1)}, E_j^{(2)}$, where $E_j^{(1)} \gg E_j^{(2)}$, such that regions with $E_j^{(2)}$ act as pinning centers. We denote the size of the pins by $s_p$ and their distance, i.e., the size of the regions with $E_j^{(1)}$, by $d_p$. Then the condition for commensurability states that the defect lattice period $d_p + s_p$ must be an integer multiple $n$ of the VL period $a$, such that the direction of the individual PF is the same for many pins [the number of pins with aligned PF is of the order of $\lambda_m/(s_p + d_p)$]

$$d_p + s_p = n a_{\mathrm{coh}} = n 2\lambda_j^{(1)} \kappa_{\mathrm{coh}} K(\kappa_{\mathrm{coh}}^2) \approx n\pi\lambda_j^{(1)} \frac{H_{c_0}^{(1)}}{H_e} \quad (n = 1,2,3,\ldots) . \tag{13}$$

Note that the most general commensurability criterion would allow $n$ to be rational, $n = q/p$, with $q$ and $p$ integer. However, only the case $p = 1$ leads to very strong pinning, since the number of pinning centers giving rise to aligned PF's is reduced by a factor $1/p$ for $p \neq 1$. Nevertheless, in Figs. 6(a)–6(c), small peaks with $p = 2$ and $q = 1,3$ can still be identified.

With the above described type of disorder, we performed simulations for various sets of parameters $d_p, s_p$. Figure 6(a) shows the experimentally measured $I_c(H_e)$,[25]

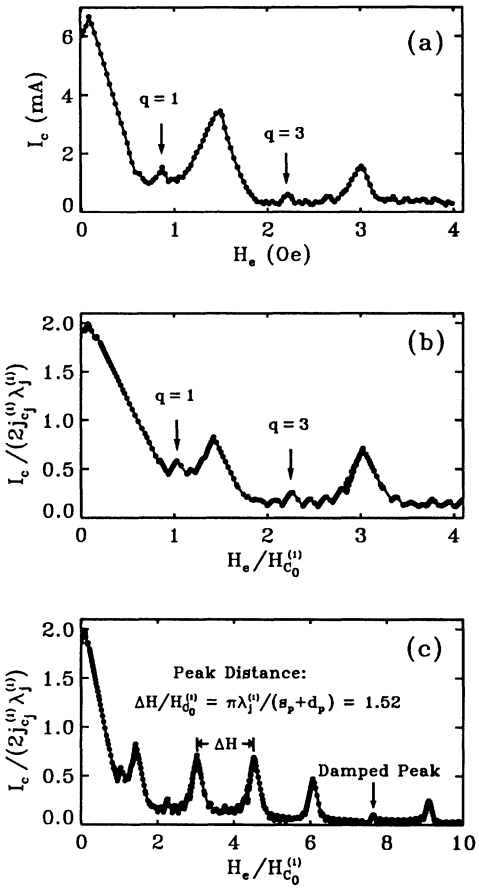


FIG. 6. A comparison between the experimentally measured field dependence of the critical current, $I_c(H_e)$, of a periodically modulated junction (Ref. 25) (a), and (b) the numerically calculated $I_c(H_e)$ of a junction with the experimental parameters, $L/\lambda_j^{(1)} \approx 18.7$, $d_p\lambda_j^{(1)} \approx 1.66$, $s_p/\lambda_j^{(1)} \approx 0.4$, and the chosen ratio $\lambda_j^{(1)}/\lambda_j^{(2)} = 0.1$. Plotting the numerically calculated $I_c$ for larger fields (c), one observes a damped peak due to a minima in the pinning force $\hat{F}_p$. The distance between the peaks confirms the commensurability criterion Eq. (13). Note also the two smaller peaks with $p = 2$ and $q = 1,3$ in (a), (b), and (c).

and in Fig. 6(b) the numerical result for $I_c(H_e)$ obtained from a simulation with the experimental parameters ($L/\lambda_j^{(1)} \approx 18.7$, $d_p/\lambda_j^{(1)} \approx 1.66$, and $s_p/\lambda_j^{(1)} \approx 0.4$) is shown. As far as we know, the value of $\lambda_j^{(2)}$ cannot be determined experimentally, but the numerical calculations show that the $I_c(H_e)$ curve is basically unaffected by a change of the ratio $\lambda_j^{(2)}/\lambda_j^{(1)}$ as long as it remains larger than approximately 2, so we arbitrarily choose $\lambda_j^{(2)}/\lambda_j^{(1)} = 10$ in all our simulations. Since, in the experiment, a symmetrical junction geometry was used, we transformed our results, which used the boundary conditions of an asymmetrical junction (see Sec. II), to the symmetrical case. One observes very good agreement between the calculated and the measured curve, and, in particular, the criterion Eq. (13) is very well confirmed by the positions of the peaks.

However, one of the peaks in the calculated curve Fig. 6(c) is almost *absent*, which at first sight seems surprising. The explanation is simple: From the calculation of the PF in Sec. III, we know that the net force vanishes if the pinning center size is an integer multiple of the VL period. For the above value of $s_p/\lambda_j^{(1)} \approx 0.4$, the corresponding field is given by $H_e/H_{c_0}^{(1)} \approx 7.9$, which coincides with the position of the damped peak. In the above mentioned experiment, $I_c$ was not measured at fields large enough so that this feature could have been observed, but, in principle, this damping should also be experimentally detectable. In Fig. 1(c), the local field and current density is plotted at the critical current with an external field $H_e/H_{c_0}^{(1)} = 5$ for a junction with parameters $L/\lambda_j^{(1)} = 10$, $d_p/\lambda_j^{(1)} = 0.6$, and $s_p/\lambda_j^{(1)} = 0.1$. One observes the above mentioned vortex density modulation, the wavelength of which determines the size of regions where the PF's are essentially adding up coherently.

For most other values of the relevant parameters $d_p, s_p$, the field dependence of $I_c$ looks qualitatively the same with one exception: If the ratio between the pinning center size $s_p$ and their distance $d_p$ is rational, i.e., $s_p/d_p = r/s$, where $r,s$ are integers, the commensurability criterion and the criterion for the vanishing of the PF coincide for all values of $n$ in Eq. (13), which satisfy the relation $n = r + s$. This suggests that the corresponding peaks should be suppressed. Figure 7 shows the calculated $I_c(H_e)$ curve for a junction with parameters $L/\lambda_j^{(1)} = 10, d_p/\lambda_j^{(1)} = s_p/\lambda_j^{(1)} = 0.4$, i.e., $r = s = 1$. One observes that the above mentioned peaks (in this particular case every other one) are indeed suppressed. The suppressed peaks obey the commensurability criterion

$$\begin{aligned} d_p + s_p &= m(r+s)a_{\mathrm{coh}} \\ &= m(r+s)2\lambda_j^{(1)}\kappa_{\mathrm{coh}}K(\kappa_{\mathrm{coh}}^2) \\ &\approx m(r+s)\pi\lambda_j^{(1)}\frac{H_{c_0}^{(1)}}{H_e} \quad (m = 1,2,3,\ldots). \end{aligned} \tag{14}$$

This example again proves that the pinning center size is a crucial parameter, and, as we shall see in the next section, this is also true for the case of random disorder, which is our main interest in the present work.

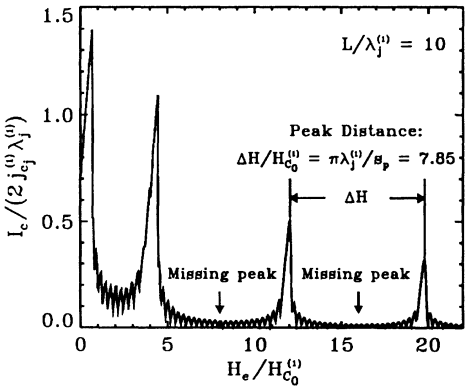


FIG. 7. The field dependence of the critical current, $I_c(H_e)$, of a periodically modulated junction with equal pinning center size $s_p$ and pinning center distance $d_p$. The parameters are $L/\lambda_j^{(1)} = 10$, $s_p/\lambda_j^{(1)} = d_p/\lambda_j^{(1)} = 0.4$, and $\lambda_j^{(1)}/\lambda_j^{(2)} = 0.1$. Note that every other peak is missing due to the vanishing PF at the fields defined from the commensurability criterion Eq. (14).

## VI. RANDOM DISORDER AND COLLECTIVE PINNING

Among the types of disorder we investigated, the random case is probably the most interesting and also the most relevant one. In general, every real sample contains some kind of randomly distributed defects, and, in particular, since the critical current of granular superconductors is believed to be limited by the current carrying capacity of its weak links, which in turn couple the single grains, the study of the pinning by random disorder could also provide insight into properties of such materials. For possible applications of granular superconductors, the critical current at large fields is of particular interest, so we intended to study its field dependence for fields $H_e \gg H_{c_0}$, where $H_{c_0} \approx 20$–$80$ G is a typical value.

For bulk type-II superconductors, it was soon realized that the nonvanishing critical current in the Abrikosov state is due to the pinning of the flux tubes at defects. A very successful theory for the description of random pinning was developed by Larkin and Ovchinnikov, the *collective pinning theory*.[10] The central idea of CPT is the assumption that the long-range order of the VL is destroyed by the presence of the disorder, leaving a short-range order over some correlation length $L_c$. The length $L_c$ depends on the elasticity of the lattice determined by the vortex-vortex interaction, and on the disorder. Each correlated volume is assumed to be pinned *independently* by a total PF, which is due to fluctuations, since the average PF of randomly positioned pinning centers vanishes. The critical current can then be estimated from the equilibrium condition between the driving Lorentz and the total PF acting on this volume.

Very recently Vinokur and Koshelev (VK) noticed that this theory might also be applied to random pinning of Josephson vortices in LJJ. They estimated the field dependence of the critical current and found that it should exhibit a *plateau* behavior for large fields, i.e.,

$j_c(H_e)$ should become a constant. Furthermore, they argued that the correlation length $L_c$ should substitute the average penetration depth $\bar{\lambda}_j$ in distinguishing the effective dimensionality of a junction, i.e., junctions with $L < L_c$ (even if $L \gg \bar{\lambda}_j$) should behave like randomly disordered point contacts, for which the effect of random disorder was investigated earlier.[14,15]

While we started numerical simulations for random pinning, we could not find the predicted plateau behavior of $j_c(H_e)$. This led us to reinvestigate the collective pinning analysis of VK and to carefully compare the prediction of CPT with the exact numerical results, since it did not seem clear *a priori* that this theory should also apply to LJJ.

The discrepancy between the prediction of VK and the simulation could soon be explained by the fact that VK did not take the importance of the average pinning center size $\bar{r}_0$ and its expected fluctuation $\sigma_{r_0}$ into account. In their formulas, they used a simple approximation for the average elementary PF of a single defect, which is only justified if $\bar{r}_0 \ll \bar{\lambda}_j$ and for fields $H_e \ll \pi \bar{\lambda}_j \bar{H}_{c_0}/\bar{r}_0$. In this parameter range, their predictions are found to be correct. The use of the exact expression (8) for the average PF extends the applicability of VK's results to arbitrary fields $H_e \geq 3\bar{H}_{c_0}$, and arbitrary junction parameters.

We checked the dependence of the formulas for $j_c$ predicted by CPT (using the exact PF) on all the parameters, and found astonishing agreement with the simulations to an accuracy given by the statistical error bars. Also the overall qualitative shape of the $j_c(H_e)$ curve is predicted correctly. The numerical factor needed to obtain quantitative agreement between the two approaches is $\approx 2$, so the order of magnitude of $j_c$ is correctly estimated by CPT.

In order to apply CPT, one needs to find an expression for the elastic modulus of the VL, which, in the one-dimensional case under consideration, is simply the compression modulus. This can be done by expanding the energy functional $E[\Theta(x)]$ to first order in the displacement field $u(x)$.[9] In our case, $u(x)$ can be introduced by writing the perturbed phase $\Theta(x)$ in terms of the slightly disturbed homogeneous phase distribution $\Theta_0(x)$

$$\Theta(x) = \Theta_0(x - u(x)) \ .$$

This is correct under the assumption of weak disorder. By inserting this ansatz into (6), VK have shown that this results in an effective functional $\tilde{E}[u(x)]$ given in terms of the displacement field $u(x)$, which for the case of one dimension becomes [$\tilde{x} = x - u(x)$]

$$\tilde{E}[u(\tilde{x})] = \int_{-u(0)}^{L-u(L)} \left[ \frac{C(\tilde{x})}{2} \left( \frac{\partial u}{\partial \tilde{x}} \right)^2 + \left( 1 + \frac{\partial u}{\partial \tilde{x}} \right) V_p(\tilde{x}+u)[1 - \cos\Theta_0(\tilde{x})] + \left( 1 + \frac{\partial u}{\partial \tilde{x}} \right) j \frac{\hbar}{2e} \Theta_0(\tilde{x}) \right] d\tilde{x} \ , \tag{15}$$

where $j$ is the external current density. The random potential $V_p(x)$ is assumed to be short range correlated according to

$$\langle V_p(x_1) V_p(x_2) \rangle = \bar{E}_j^2 q e^{-|x_1 - x_2|/\bar{r}_0} \ ,$$

where $\bar{E}_j$ is the average Josephson coupling energy, $q = \langle \delta j_{c_j}^2 \rangle / \bar{j}_{c_j}^2 \ll 1$ describes the strength of the disorder, and the typical length scale of the disorder is the average pin size $\bar{r}_0$ with variance $\sigma_{r_0}$. The resulting elementary PF can thus be approximated by $\bar{F}_p$ from Eq. (10). The compression modulus is the coefficient of the elastic term in Eq. (15), and is given by

$$C(\tilde{x}) = \bar{E}_j \bar{\lambda}_j^2 \left( \frac{\partial \Theta_0}{\partial \tilde{x}} \right)^2 \propto 4\bar{E}_j \left( \frac{H_e}{\bar{H}_{c_0}} \right)^2 = \text{const} \ ,$$

where $\bar{\lambda}_j, \bar{H}_{c_0}$ are again average values, and the asymptotic result holds in the large field limit. Following CPT, one is now in the position to estimate the correlation length $L_c$ by minimizing the sum of the elastic and the pinning energy of a correlated region with respect to its size. $L_c$ is determined by the condition that the variation of the displacement $u$ along the correlated region is of the order of the length scale of the effective pinning potential. Since this potential varies on the scale of the VL period $a$ (see Sec. III), the gradient $\partial u / \partial \tilde{x}$, which enters the elastic energy, can be approximated by its average $a/L_c$ across the correlation volume. The pinning energy is calculated by adding the *random* PF's in the *finite* volume $L_c$, and is proportional to the square root of the number of pinning centers in $L_c$. The relevant energy density is therefore

$$E_c(L_c) \approx \frac{C(\tilde{x})}{2} \left( \frac{a}{L_c} \right)^2 - \bar{F}_p \bar{E}_j q^{1/2} a \left( \frac{n}{L_c} \right)^{1/2} \ ,$$

where the defect concentration is defined by $n = 1/\bar{r}_0$. The total average PF acting on the correlation volume is assumed to be zero, so the actual pinning arises from fluctuations resulting in a pinning energy proportional to the square root of the pinning-center density. Since we are only interested in the behavior for moderate to large fields $H_e/\bar{H}_{c_0} \geq 3$, in the following calculations, we always use the asymptotic values for the compression modulus $C(x)$ (see above) and the VL period $a \propto \pi \bar{\lambda}_j \bar{H}_{c_0}/H_e$. From the minimization we then obtain

$$L_c \approx 4\pi \bar{\lambda}_j \left( \frac{\bar{r}_0}{\pi q \bar{\lambda}_j} \right)^{1/3} \left( \frac{H_e}{\bar{H}_{c_0} \bar{F}_p} \right)^{2/3} \ . \tag{16}$$

In contrast to the prediction of VK, $L_c$ is not independent of field, but *increases* as $H_e^{2/3}$ at large fields, for which the pinning force becomes effectively constant. Since CPT assumes each correlation volume to be pinned independently, the critical current is determined from the equilibrium condition between pinning and Lorentz force

density for a single volume of size $L_c$

$$\frac{1}{c} j_c H_e = \bar{F}_p \bar{E}_j q^{1/2} \left[ \frac{n}{L_c} \right]^{1/2} . \tag{17}$$

Note that our $j_c$ has a dimension current per length, because we set the junction width $W=1$. At this point, one has to distinguish the dimensionality of the junction: If $L < L_c$ the short-range order of the VL extends across the entire junction. This means that the pinning of *all* the vortices is correlated and $L_c$ must be substituted by the junction length $L$ in Eq. (17). Thus $L_c$ is a new *effective length scale,* which distinguishes short [zero-dimensional (0D)] and long [one-dimensional (1D)] randomly disordered Josephson junctions, replacing the corresponding length $\bar{\lambda}_j$, which plays this role for a homogeneous junction. This has an important consequence: As mentioned above, $L_c$ increases with field, which means that for a junction with $L > L_c$ at $H_e = 0$, there exists a critical field $H_{c_L}$ for which $L = L_c$, and hence for fields $H_e > H_{c_L}$, a *dimensional crossover* takes place from one- to zero-dimensional behavior of the junction. This crossover could not be obtained using the approximation of VK. Again using the asymptotic expressions, the final formulas for the critical current density of the short and long junction read

$$L > L_c: \; j_c \approx \frac{\bar{j}_{c_j}}{4\pi} \left[ \frac{\pi q \bar{\lambda}_j}{\bar{r}_0} \right]^{2/3} \left[ \frac{\bar{F}_p \bar{H}_{c_0}}{H_e} \right]^{4/3} \propto \left[ \frac{\bar{H}_{c_0}}{H_e} \right]^{4/3} \quad (H \gg H_\sigma) , \tag{18a}$$

$$L < L_c: \; j_c \approx \frac{\bar{j}_{c_j}}{2} \left[ \frac{q \bar{\lambda}_j^2}{\bar{r}_0 L} \right]^{1/2} \frac{\bar{F}_p \bar{H}_{c_0}}{H_e} \propto \frac{\bar{H}_{c_0}}{H_e} \quad (H \gg H_\sigma) . \tag{18b}$$

For large fields $H_e \gg H_\sigma = \pi \bar{H}_{c_0} \bar{\lambda}_j / \sigma_{r_0}$, the PF $\bar{F}_p$ becomes constant, and one obtains the above asymptotic field dependence. It is important to keep in mind that Eqs. (18a) and (18b) only represent a *dimensional estimate,* so that one should not expect the numerical values of $j_c$ calculated from these formulas to be exact. However, the functional dependence on the given parameters can be assumed to be correct, if CPT is a valid approach. The expressions Eqs. (18) are amenable to a direct check by our numerical simulations. The dependence of $j_c$ on the parameters $q$ and $L$, and also its asymptotic field dependence can be directly extracted from the simulations because it is a simple power law. The dependence on $\bar{r}_0$ and $\sigma_{r_0}$ is not explicitly given, since the PF also depends on them. Therefore, one can only check the qualitative agreement between the numerically calculated $j_c(H_e)$ curve, and the one predicted from CPT for a set of values of this parameters. In Fig. 1(d), we show a typical plot of the coupling $E_j(x)$, as well as $j(x)$, and $H(x)$ at the critical current for applied field $H_e/\bar{H}_{c_0} = 5$, and junction parameters $q = 0.09$, $\bar{r}_0/\bar{\lambda}_j = 0.1$, $\sigma_{r_0}/\bar{\lambda}_j = 0.02$, $L/\bar{\lambda}_j = 10$. One observes the existence of an average (Bean critical state) gradient $\partial H/\partial x$, which is responsible for the finite average critical current density. This is completely analogous to a critical state in type-II superconductors.[3]

Before reporting our numerical results, we need to say a few words about the algorithm for the calculation of $j_c$ in the presence of random disorder: The disorder is again modeled by choosing $E_j(x)$ to be a piecewise constant function where the lengths $l^{(i)}$ of the constant regions as well as the corresponding values $E_j^{(i)}$ are random Gaussian deviates with mean values $\bar{E}_j, \bar{r}_0$ respectively. The variance of $E_j^{(i)}$ is determined from the variance $q$ of $j_c^{(i)}$, and the variance of $l^{(i)}$ is $\sigma_{r_0}$. For each such obtained realization of the junction, the critical current is calculated as described in Sec. II, and finally, a statistical average of $j_c$ is taken over many ($N$) realizations. The statistical error is given by the standard deviation $\sigma_{j_c}$ of $j_c$, renormalized by the square root of the number of realizations: $\Delta j_c = \sigma_{j_c}/\sqrt{N}$. In order to keep the error bars and the computing time reasonably small, we typically used 100–300 realizations resulting in a typical relative error of less than 3%.

The check of the $q$ and $L$ dependence was done for a junction with parameters $\bar{r}_0/\bar{\lambda}_j = 0.05$, $\sigma_{r_0}/\bar{\lambda}_j = 0.01$, and a field of $H_e/\bar{H}_{c_0} = 80$. Figure 8(a) shows a plot of $I_c$ vs $L^{1/2}$. One observes the expected linear increase for small values of $L$ (i.e., $j_c \propto L^{-1/2}$ as predicted for a short junction) up to a length $L_c/\bar{\lambda}_j \approx 35$ from where the curve is starting to bend away towards a quadratic behavior at larger $L$. This proves the existence of the above mentioned crossover from zero- to one-dimensional behavior, i.e., $I_c \propto L$ for larger $L$. The length at which the crossover occurs should correspond to the correlation length, which for this junction and field was estimated to be $L_c/\bar{\lambda}_j \approx 100$. This means that the numerical factor in the estimate Eq. (16) is $\approx 0.35$. However, one has to take into account that it is not possible to obtain a very accurate value of $L_c$ from the numerical $I_c(L)$ dependence, since the size of the region of crossover is not well defined. In summary, these results prove the existence of a critical current *density* for one-dimensional LJJ's and hence show that a collective pinning approach to the random pinning problem of the LJJ is possible. For the zero-dimensional case, $j_c$ is not a true current density since it is a length-dependent quantity.

The values of $j_c$ extracted from the slopes of $I_c$ in the two regimes depicted in Figs. 8(a) and 8(b) confirm that the numerical factor needed to match the predictions from Eqs. (18) and the numerical results is $\approx 2$: For the 1D regime one extracts $j_c^{\text{num}}/\bar{j}_{c_j} \approx 0.93 \times 10^{-3}$ compared

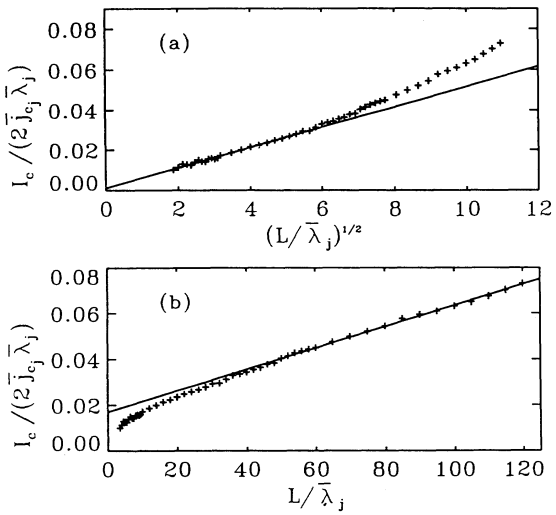


FIG. 8. The length dependence of the critical current, $I_c$, of a randomly disordered junction with parameters $q=0.09$, $\bar{r}_0/\bar{\lambda}_j=0.05$, $\sigma_{r_0}/\bar{r}_0=0.2$, and fixed applied field $H_e/\bar{H}_{c_0}=80$: (a) A plot of $I_c$ vs $L^{1/2}$. One observes a linear rise for small $L/\bar{\lambda}_j \leq 35$, indicating the law $I_c \propto L^{1/2}$, characteristic for a 0D junction, i.e., $L > L_c$. (b) The same data $I_c$ plotted vs $L$. From the value $L/\bar{\lambda}_j \approx 35$, a linear rise sets in, confirming the existence of a critical current density, which is predicted by CPT for a 1D junction. The critical value $L_c/\bar{\lambda}_j \approx 35$ is therefore an estimate of the CPT correlation length at this field.

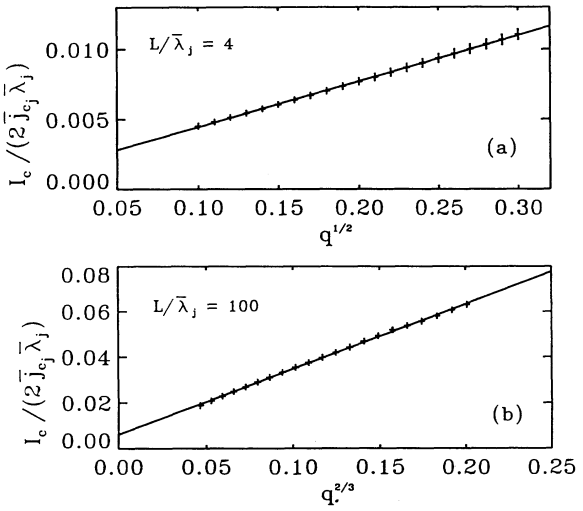


FIG. 9. The dependence of the critical current $I_c$ on the strength $q$ of the disorder at the field $H_e/\bar{H}_{c_0}=80$ for the same junction as in Fig. 8. (a) A plot of $I_c$ vs $q^{1/2}$ for a junction length $L/\bar{\lambda}_j=4$, i.e., a 0D junction. The observed straight line confirms the proportionality $I_c \propto q^{1/2}$, predicted by CPT [Eq. (18b)]. (b) A plot of $I_c$ vs $q^{2/3}$ for a junction length $L/\bar{\lambda}_j=100$, i.e., a 1D junction. In this case, the observed straight line confirms the proportionality $I_c \propto q^{2/3}$, predicted by CPT [Eq. (18a)].

to the predicted $j_c^{\mathrm{CPT}}/\bar{j}_{c_j} \approx 0.57\times10^{-3}$, and for the 0D regime we obtain $L^{1/2}j_c^{\mathrm{num}}/\bar{j}_{c_j} \approx 1.01\times10^{-2}$ compared to $L^{1/2}j_c^{\mathrm{CPT}}/\bar{j}_{c_j} \approx 7.0\times10^{-3}$. Note also that the current extrapolates nicely to zero for $L \to 0$.

Figures 9(a) and 9(b) show a plot of $j_c$ vs $q^{1/2}$ of the same junction with length $L/\bar{\lambda}_j=4$, i.e., the 0D case, and vs $q^{2/3}$ with length $L/\bar{\lambda}_j=100$, i.e., the 1D case. Both points fit perfectly well to a straight line within the error bars, and in the limit $q \to 0$ both curves extrapolate nicely to the values obtained for the corresponding homogeneous junction. Of course, a dependence of $q^{1/2}$ is very hard to distinguish from $q^{2/3}$ if represented by a finite number of points, but the fit with the predicted exponent was better in both cases. So the $q$ and $L$ dependence of $j_c$ is confirmed by the simulations.

Another feature we observed in the length-dependent calculations was that the relative variance of the critical current $\sigma_{j_c}/j_c$, decreased with increasing length of the junction. This is quite important in view of the relevance of this theory to the polycrystalline high-$T_c$ materials: Experimentally it is observed that the fluctuations in the critical current of different ceramic samples produced under equivalent conditions are very small.[27] If we assume that the critical current in such systems is limited by the depinning across a critical path of macroscopic length,[17] i.e., an inhomogeneous LJJ, this experimental finding corresponds to a relative variance in the calculated values of $j_c$ from different realizations of the disorder, which should scale to zero as the junction length increases. This self-averaging effect agrees with the results of our simulations.

From the physical point of view, the most interesting property of the junction is the field dependence of the critical current. Figures 10(a)–10(d) show numerically obtained $j_c(H_e)$ curves for disorder strength $q=0.09$ and several different sets of parameters $\bar{r}_0/\bar{\lambda}_j$ and $L/\bar{\lambda}_j$ compared to the corresponding curves calculated with CPT for the same parameters. The ratio $\sigma_{r_0}/\bar{r}_0=0.2$ was identical for all four junctions. The basic features we observe are (i) the increase of the Meissner peak at $\bar{H}_{c_0}$ and its shift to larger fields $H_e/\bar{H}_{c_0} \approx 2-3$ for large-scale disorder, (ii) the appearance of a plateau with almost field independent $j_c$ for disorder with length scale $\bar{r}_0/\bar{\lambda}_j < 0.2$, and (iii) the formation of a local minimum at the field $H_{\bar{r}_0} \approx (\pi\bar{\lambda}_j/\bar{r}_0)\bar{H}_{c_0}$ at which the VL period coincides with the average defect size. Comparing the numerical curves with the predicted ones shows that features (ii) and (iii) are both perfectly reproduced and also the overall shape of the curves agrees beautifully. The Meissner-peak is not found in the CPT results, since we restricted ourselves to fields $H_e/\bar{H}_{c_0} \geq 3$ in our analysis. The curves estimated by CPT were rescaled by a factor of $\approx 2$ in order to allow a comparison of the qualitative shapes with the numerical results. This value represents the numerical factor mentioned above. The asymptotic field dependence of $j_c$ calculated for a junction with parameters $q=0.09$, $\bar{r}_0/\bar{\lambda}_j=0.5$, $L/\bar{\lambda}_j=200$, and $\sigma_{r_0}/\bar{r}_0=0.2$ is depicted in Fig. 11. One can nicely observe the crossover

from 1D to 0D behavior at a field $H_e/\bar{H}_{c_0} \approx 80$, where the field dependence changes from $j_c \propto H_e^{-4/3}$ to $j_c \propto 1/H_e$.

The effect of different ratios $\sigma_{r_0}/\bar{r}_0$ is demonstrated in Fig. 12. If the ratio is zero, one can nicely observe the effect of the oscillatory behavior due to the periodic unaveraged elementary PF $\hat{F}_p$, Eq. (9). For small values of $\sigma_{r_0}/\bar{r}_0$, a few peaks still survive, whereas for values $\sigma_{r_0}/\bar{r}_0 > 0.2$, only the first peak is observable. Note that for fields $H_e < H_{\bar{r}_0}$, all the curves essentially coincide. This behavior directly reflects the field dependence of the averaged pinning force $\bar{F}_p$, which was shown for different ratios $\sigma_{r_0}/\bar{r}_0$ in Fig. 4.

Another point to mention is that the presented graphs always show the average value of $j_c$, which can be thought of as a background current produced by the random pinning. Superimposed on this background, one has to imagine the characteristic oscillatory structure of the homogeneous $I_c(H)$ dependence resulting from the formation of an additional vortex. This oscillatory structure is seen in the numerical calculations when considering the critical current of a single realization of the disorder, but it disappears upon averaging.

From the presented results, one finds the important conclusion that the critical current can be kept at a considerably large value for increasing field as long as the length scale of the disorder is very small compared to the penetration depth. The dramatic drop in $j_c$ occurs at the above mentioned field $H_{\bar{r}_0} \approx (\pi\bar{\lambda}_j/\bar{r}_0)\bar{H}_{c_0}$. For fields above this threshold value, the pinning is drastically reduced. However, it still leads to a nonzero critical current *density* (for the 1D case), in contrast to a homogeneous junction.

## VII. CONCLUSIONS

We have presented a detailed study of Josephson vortex pinning in one-dimensional inhomogeneous LJJ with various types of disorder. The critical current of the disordered LJJ was calculated as a function of the applied magnetic field, (i) numerically by exactly solving the *self-consistent* stationary sine-Gordon equation in the presence of a piecewise constant maximum Josephson current

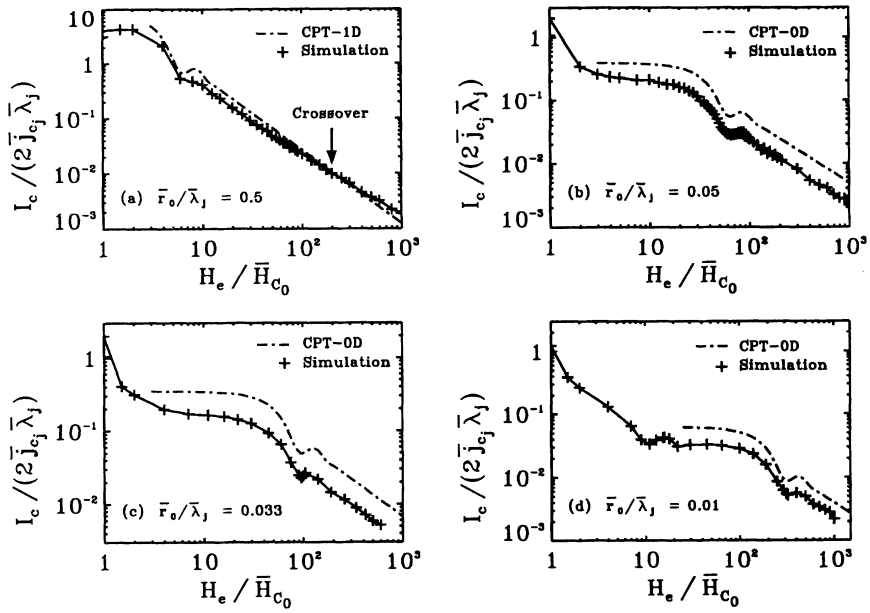


FIG. 10. A comparison between the predicted (CPT) and the numerically determined field dependence of the critical current, $I_c(H_e)$, for four randomly disordered junctions with different parameters $\bar{r}_0/\bar{\lambda}_j$, and $L/\bar{\lambda}_j$, but with the same values $q=0.09$, and $\sigma_{r_0}/\bar{r}_0=0.2$. (a) A junction with large scale disorder $\bar{r}_0/\bar{\lambda}_j=0.5$, and $L/\bar{\lambda}_j=200$. No plateau is found, and from the field $H_e/\bar{H}_{c_0}\approx 10$, the asymptotic decrease $I_c \propto H_e^{-4/3}$ sets in, until $H_e/\bar{H}_{c_0}\approx 70$, where a crossover to the behavior $I_c \propto H_e^{-1}$, characteristic for 0D junctions, is observed. The sharp drop in $I_c$ usually found at $\bar{H}_{c_0}$ is shifted to larger fields $\approx 3\bar{H}_{c_0}$. (b) A junction with a smaller disorder length scale $\bar{r}_0/\bar{\lambda}_j=0.05$, and length $L/\bar{\lambda}_j=30$. A plateau is observed for fields $H_e/\bar{H}_{c_0}\leq 20$, followed by the characteristic minimum when the vortex spacing $a$ is equal to $\bar{r}_0$ (at $H_e/\bar{H}_{c_0}\approx 60$), and finally, the asymptotic (0D) decrease $I_c \propto H_e^{-1}$. (c) A junction with a disorder length scale $\bar{r}_0/\bar{\lambda}_j=0.033$, and length $L/\bar{\lambda}_j=30$. The graph is qualitatively the same as in (b). However, the observed plateau is slightly lower than in (b), and extends to larger fields $H_e/\bar{H}_{c_0}\leq 35$. (d) A short junction with a small disorder length scale $\bar{r}_0/\bar{\lambda}_j=0.01$, and length $L/\bar{\lambda}_j=6$. The drop of $I_c$ at $H_e=\bar{H}_{c_0}$ has become much smoother, and is followed by a small maximum on the plateau. The plateau itself extends to large fields $H_e/\bar{H}_{c_0}\approx 110$, and the characteristic minimum is at $H_e/\bar{H}_{c_0}\approx 310$. Note that the statistical error bars are smaller than the data symbols in all cases.

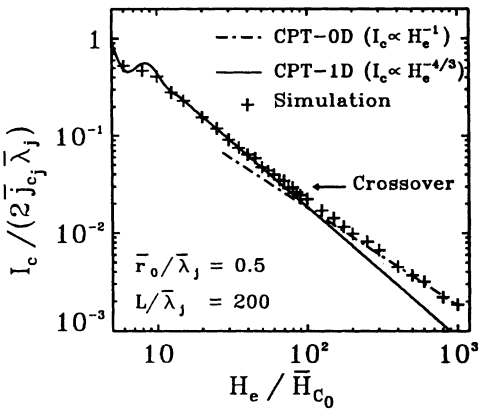


FIG. 11. The dimensional crossover shown in Fig. 10(b). The numerically obtained data points are compared, (i) against the prediction for a 1D junction, and (ii) against the prediction for a 0D junction. One observes that for small fields ($H_e/\bar{H}_{c_0} \leq 60$) the 1D prediction gives the correct asymptotic decrease, whereas for ($H_e/\bar{H}_{c_0} \geq 200$) the 0D prediction is correct.

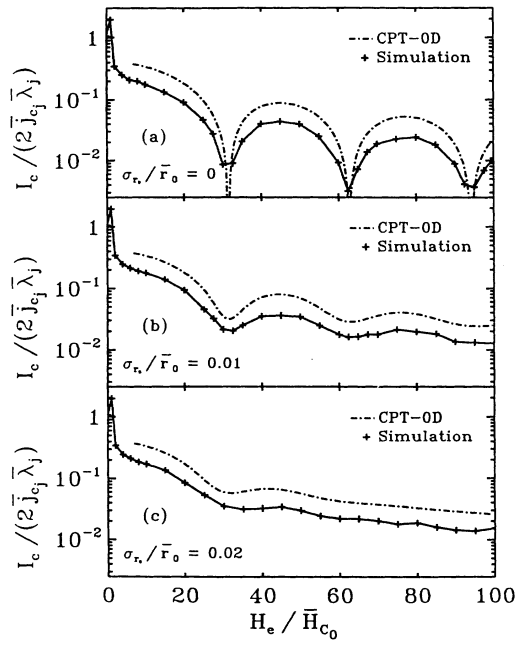


FIG. 12. The effect of a varying pin size randomness $\sigma_{r_0}/\bar{r}_0$ on the field dependence of the critical current $I_c$ for junctions with $q=0.09$, $\bar{r}_0/\bar{\lambda}_j=0.1$, and $L/\bar{\lambda}_j=20$. (a) Equal pinning center sizes, $\sigma_{r_0}=0$. Sharp minima are observed at field values where the averaged PF vanishes, i.e., the pin size $\bar{r}_0$ is an integer multiple of the vortex spacing $a$ (see Fig. 4). (b) The minima of the junction with $\sigma_{r_0}/\bar{r}_0=0.1$ are strongly smoothed, and disappear for large fields. (c) At $\sigma_{r_0}/\bar{r}_0=0.2$, only the first minimum (at $H_e/\bar{H}_{c_0}\approx 30$) survives, and for large fields, the smooth asymptotic decrease $I_c \propto H_e^{-1}$ predicted for a 0D junction is found.

density $j_{c_j}(x)$ and (ii) for the case of random pinning, by extending the collective pinning analysis[9] by VK to arbitrary external fields and junction parameters.

Our main achievement was to show that CPT provides an excellent qualitative description of random disorder in LJJ. The crucial quantity which enters CPT is the average elementary PF. In contrast to VK, who used a simple approximation, we have calculated this force analytically, and as a consequence, using CPT, many additional features in the field dependence of the critical current were predicted, and also verified in the comparison to the numerical results. In particular, the existence of a critical current *density* $j_c$, which is a necessary condition for CPT, has been shown by numerical investigation of the length dependence of the critical current, in contrast to the uniform junction, which is only able to carry a surface current.

One of the main results of VK was the substitution of $\bar{\lambda}_j$ by the CPT correlation length $L_c$ as the length scale distinguishing between the effective dimensionality of the junction: For junction length $L > L_c$, there should be 1D, for $L < L_c$, 0D behavior (as for a randomly disordered Josephson point contact). This finding is confirmed by our results. However, we discovered an additional feature: The approximation of VK yielded a field-independent value of $L_c$ for large fields, whereas by using the exact PF, we obtained the result that $L_c$ increases with a power law $\propto H_e^{2/3}$. This means that a junction, which behaves effectively one dimensionally at low fields, will show a *dimensional crossover* to a point contact as the field increases.

Within their approximation, VK obtained a constant critical current density for arbitrary large fields. We have shown that this approximation is only valid for disorder that varies on length scales $\bar{r}_0$ much smaller than the average Josephson penetration depth $\bar{\lambda}_j$, and even in this case it cannot be justified as soon as the vortex spacing becomes of the order of $\bar{r}_0$. This situation arises for applied fields $H_e/\bar{H}_{c_0} \approx \pi\bar{\lambda}_j/\bar{r}_0$, and for larger values, a power-law decrease $\propto 1/H_e$ for point contacts, and $\propto H_e^{-4/3}$ for the one-dimensional case is found. This decrease is due to the fact that the PF approaches a constant value for large fields, whereas the Lorentz force increases.

This behavior shows a strong resemblance with measured $j_c(H_e)$ curves of polycrystalline high-$T_c$ superconductors: A sharp decrease of $j_c$ is found at applied fields $H_e \approx 20$–$80$ G (depending on the material and temperature),[11–13] which corresponds to the critical field $\bar{H}_{c_0}$ of the weak links in these materials. This sharp drop is followed by a large region (up to applied fields of the order of $10^4$ G at temperature $T=77$ K, and $10^5$ G at $T=4$ K) in which $j_c$ is essentially field independent. Assuming that the critical current is limited by the depinning of Josephson vortices along a critical path (a macroscopically long junction), e.g., in the context of a limiting path model,[17] one can explain these experiments as follows: If we assume that the effect of finite temperature (recall that our analysis is strictly valid only at $T=0$) is simply to

change the value of the effective parameters $\bar{\lambda}_j, \bar{H}_{c_0}, \bar{j}_{c_j}$, i.e., we neglect thermal depinning and flux creep (which is reasonable),[9] the observed plateaus could be due to very small scale disorder $\bar{r}_0 \approx 50$ Å. This estimate is obtained in the following way: In our analysis the second drop of $j_c(H_e)$ occurs when the vortex spacing $a$ is of the same order as $\bar{r}_0$. This "critical" spacing $a_d$ can be calculated from the experimental values of the field at the drop $H_d \approx 10^4$ G and the London penetration depth $\lambda_{L_0} \approx 2000$ Å (both at 77 K) as $\bar{r}_0 \approx a_d \approx \Phi_0/(H_e 2\lambda_L) \approx 50$ Å. The Josephson critical current density at this temperature can be estimated to be approximately $\bar{j}_{c_j} \approx 5 \times 10^5$ A/cm$^2$. Using these values, one can calculate the critical current density $j_c$ from Eqs. (18), and obtain the result $j_c \approx 100$ A/cm$^2$, which is in reasonable agreement with the experimental values. The scale $\bar{r}_0 \approx 50$ Å seems to suggest that the disorder in the grain boundaries could have the same origin as in the grains, viz., oxygen vacancies, with the difference that it might be stronger in the boundaries than in the grains. The change of the parameters due to the increased temperature could explain the shift of the second drop to lower fields, which is experimentally found at $T = 77$ K. However, in the above discussion, one has to bear in mind that the experimentally measured plateau persists far beyond $H_{c_1} \approx 500$ G, so Abrikosov vortices have entered the grains, and therefore one cannot say with certainty that their interaction with the Josephson vortices can be neglected. Nevertheless, the pinning of the Josephson vortices can be assumed to be much weaker than the pinning of the Abrikosov vortices, and therefore the limitation of the critical current should still be determined by the pinning strength of the Josephson vortices; i.e., our analysis should apply.

For a junction with a periodic defect lattice, our numerical results reproduced the measured peaks in the $I_c(H)$ curves[25] and the explanation for the occurrence of the peaks was confirmed to be given by the commensurability criterion between the pinning center lattice and the vortex period, as suggested earlier.[19] However, due to the behavior of the elementary pinning force, we predict the absence of peaks at fields for which the pinning center *size* is commensurate with the vortex size. Such a situation occurs whenever the ratio between the pinning center size and the pinning center distance is a rational number. This cancellation effect remains to be seen experimentally.

Finally we reported the possibility of constructing a junction with maximal pinning consisting of alternating regions with large and small Josephson coupling $E_j$. The sizes of the regions were chosen such that the critical current was maximal for a given applied field $H_{\rm opt}$ due to the exact matching between the defects and the vortex lattice. We calculated the field dependence of $I_c$ for such a junction, and found a linear increase up to the field $H_{\rm opt}$ followed by a sharp drop to values typical for corresponding uniform junctions. In the asymptotic regime of large fields, an average critical current density $j_c^{\rm opt} = (1/\pi) j_{c_j}^{(1)}$ was found, which is of the order of the maximum Josephson current density in the regions with the larger coupling. It would be interesting to see whether such a junction can actually be produced, and perhaps it could even be useful for technical applications.

Future work on disordered LJJ should certainly concentrate on the investigation of dynamic properties, such as current-voltage characteristics, especially for the case of random disorder, about which still little is known, whereas dynamic phenomena in the presence of periodic defects have already been studied fairly intensively.[7]

## ACKNOWLEDGMENTS

We wish to thank M. V. Feigelman, A. I. Larkin, A. C. Mota, J. Rhyner, and V. M. Vinokur for illuminating discussions. In particular, we are indebted to T. M. Rice for his support and helpful discussions. Two of us (R.F. and V.B.G.) acknowledge financial support from the Swiss National Foundation.

[1] B. D. Josephson, Phys. Lett. **1**, 251 (1962).
[2] A. Barone and G. Paterno, *Physics and Applications of the Josephson Effect* (Wiley-Interscience, New York, 1982).
[3] C. P. Bean, Phys. Rev. Lett. **8**, 250 (1962).
[4] O. Pla and F. Nori, Phys. Rev. Lett. **67**, 919 (1991).
[5] C. S. Owen and D. J. Scalapino, Phys. Rev. **164**, 538 (1967).
[6] K. Schwidtal and R. D. Finnegan, Phys. Rev. B **2**, 148 (1970).
[7] For a recent review, see e.g., Yu.S. Kivshar and B. A. Malomed, Rev. Mod. Phys. **61**, 763 (1989).
[8] S. A. Vasenko, K. K. Likharev, and V. K. Semenov, Zh. Eksp. Teor. Fiz. **81**, 1444 (1981) [Sov. Phys. JETP **54**, 766 (1981)].
[9] V. M. Vinokur and A. E. Koshelev, Zh. Eksp. Teor. Fiz. **97**, 976 (1990) [Sov. Phys. JETP **70**, 547 (1990)].
[10] A. I. Larkin and Yu.N. Ovchinnikov, J. Low. Temp. Phys. **34**, 409 (1979).
[11] J. W. Ekin, in *Proceedings of ICTPS 90 International Conference on "Transport Properties of Superconductors," Rio de Janeiro, Brazil 1990,* edited by R. Nicolsky (World Scientific, Singapore, 1991), p. 23.
[12] G. Paterno *et al.*, Appl. Phys. Lett. **53**, 609 (1988).
[13] H. Küpfer *et al.*, Z. Phys. B **71**, 4821 (1988).
[14] K. Yanson, Zh. Eksp. Teor. Fiz. **58**, 1497 (1970) [Sov. Phys. JETP **31**, 800 (1970)].
[15] A. Barone, G. Paterno, M. Russo, and R. Vaglio, Zh. Eksp. Teor. Fiz. **74**, 1483 (1978) [Sov. Phys. JETP **47**, 776 (1978)].
[16] For a review, see M. Tinkham and C. J. Lobb, in *Solid State Physics,* edited by H. Ehrenreich and D. Turnbull (Academic, New York, 1989), Vol. 42, p. 91.
[17] J. Rhyner and G. Blatter, Phys. Rev. B **40**, 829 (1989).
[18] H. J. Jensen, A. Brass, Y. Brechet, and A. J. Berlinsky, Cryogenics **29**, 367 (1989).
[19] I. L. Serpuchenko, B. A. Malomed, and A. V. Ustinov, Fiz. Nizk. Temp. **15**, 1128 (1989) [Sov. J. Low. Temp. Phys. **15**, 622 (1989)]; I. L. Serpuchenko and A. V. Ustinov, Solid State Commun. **68**, 693 (1988).
[20] For a discussion of different types of boundary conditions, see Ref. 2.
[21] M. Abramowitz and I. A. Stegun, *Handbook of Mathematical Functions* (Dover, New York, 1965).
[22] W. H. Press, B. P. Flannery, S. A. Teukolsky, and W. T.

Vetterling, *Numerical Recipes* (Cambridge University Press, Cambridge, England, 1986).

[23]A. A. Golubov, I. L. Serpuchenko, and A. V. Ustinov, Zh. Eksp. Teor. Fiz. **94**, 297 (1988) [Sov. Phys. JETP **67**, 1256 (1988)].

[24]M. L. Kulić, Solid State Commun. **63**, 537 (1987).

[25]V. A. Oboznov and A. V. Ustinov, Phys. Lett. A **139**, 481 (1989).

[26]A more detailed analysis of these phenomena is planned to be published elsewhere.

[27]H. Dersch (private communication).

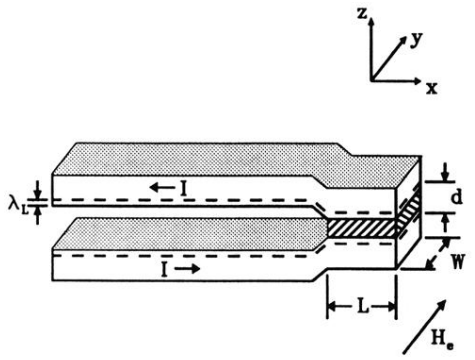


FIG. 2. The geometry of the "in-line asymmetrical" LJJ.

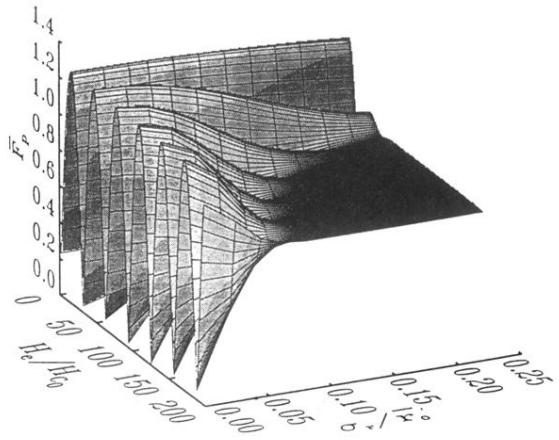


FIG. 4. The averaged pinning force $\bar{F}_p$ of a single defect as a function of the parameter $\kappa^{-1}(\propto H_e/H_{c_0}$ for $H_e/H_{c_0}\gg 1)$, and the degree of randomness of the distribution of the pin size, $\sigma_r/\bar{r}_0'$. The average pinning center size is chosen as $\bar{r}_0/\bar{\lambda}_j=0.1$. As the randomness is turned on, the oscillatory structure of $\bar{F}_p$ found for fixed pinning center size ($\sigma_r/\bar{r}_0'=0$) is smoothed out, and for large fields, $\bar{F}_p$ approaches a constant. For $\sigma_r/\bar{r}_0'\geq 0.2$, only the first minima at the field where the average pinning center size $\bar{r}_0$ is equal to the vortex spacing $a$ survives. The regime of constant pinning force corresponds to the asymptotic decrease of the critical current stated in Eqs. (18).